

Understanding the transfer of contemporary temperature signals into lake sediments via paired oxygen isotope ratios in carbonates and diatom silica: Problems and potential

David B. Ryves^{a,*}, Melanie J. Leng^{b,c}, Philip A. Barker^d, Andrea M. Snelling^{a,b,1}, Hilary J. Sloane^b, Carol Arrowsmith^b, Jonathan J. Tyler^{e,2}, Daniel R. Scott^a, Alan D. Radbourne^{a,3}, N. John Anderson^a

^a Geography and Environment, Loughborough University, Loughborough LE11 3TU, UK

^b NERC Isotope Geosciences Facilities, British Geological Survey, Keyworth, Nottingham NG12 5GG, UK

^c Centre for Environmental Geochemistry, School of Biosciences, Sutton Bonington Campus, University of Nottingham, Loughborough LE12 5RD, UK

^d Lancaster Environment Centre, Lancaster University, Lancaster LA1 4YQ, UK

^e Department of Earth Sciences, University of Oxford, Oxford OX1 3AN, UK

ARTICLE INFO

Editor: Michael E. Boettcher

Keywords:

Rostherne Mere
Sediment trap
Silica
Taphonomy
Isotope systematics
Dissolution

ABSTRACT

Although the oxygen isotope composition ($\delta^{18}\text{O}$) of calcite ($\delta^{18}\text{O}_{\text{calcite}}$) and, to a lesser extent, diatom silica ($\delta^{18}\text{O}_{\text{diatom}}$) are widely used tracers of past hydroclimates (especially temperature and surface water hydrology), the degree to which these two hosts simultaneously acquire their isotope signals in modern lacustrine environments, or how these are altered during initial sedimentation, is poorly understood. Here, we present a unique dataset from a natural limnological laboratory to explore these issues. This study compares oxygen and hydrogen isotope data ($\delta^{18}\text{O}$, $\delta^2\text{H}$) of contemporary lake water samples at ~ 2 -weekly intervals over a 2-year period (2010–12) with matching collections of diatoms ($\delta^{18}\text{O}_{\text{diatom}}$) and calcite ($\delta^{18}\text{O}_{\text{calcite}}$) from sediment traps (at 10 m and 25 m) at Rostherne Mere (maximum depth 30 m), a well-monitored, eutrophic, seasonally stratified monomictic lake in the UK. The epilimnion shows a seasonal pattern of rising temperature and summer evaporative enrichment in ^{18}O , and while there is a temperature imprint in both $\delta^{18}\text{O}_{\text{diatom}}$ and $\delta^{18}\text{O}_{\text{calcite}}$, there is significant inter-annual variability in both of these signals. The interpretation of $\delta^{18}\text{O}_{\text{diatom}}$ and $\delta^{18}\text{O}_{\text{calcite}}$ values is complicated due to in-lake processes (e.g. non-equilibrium calcite precipitation, especially in spring, leading to significant $^{18}\text{O}_{\text{calcite}}$ depletion), and for $\delta^{18}\text{O}_{\text{diatom}}$, by post-mortem, depositional and possibly dissolution or diagenetic effects. For 2010 and 2011 respectively, there is a strong temperature dependence of $\delta^{18}\text{O}_{\text{calcite}}$ and $\delta^{18}\text{O}_{\text{diatom}}$ in fresh trap material, with the fractionation slope for $\delta^{18}\text{O}_{\text{diatom}}$ of ca. $-0.2\text{‰}/^\circ\text{C}$, in agreement with several other studies. The $\delta^{18}\text{O}_{\text{diatom}}$ data indicate the initiation of rapid post-mortem secondary alteration of fresh diatom silica (within ~ 6 months), with some trap material undergoing partial maturation in situ. Diatom $\delta^{18}\text{O}$ of the trap material is also influenced by resuspension of diatom frustules from surface sediments (notably in summer 2011), with the net effect seen as an enrichment of deep-trap $^{18}\text{O}_{\text{diatom}}$ by about $+0.7\text{‰}$ relative to shallow-trap values. Contact with anoxic water and anaerobic bacteria are potentially key to initiating this silica maturation process, as deep-trap samples that were removed prior to anoxia developing do not show enrichment. Dissolution (perhaps enhanced by anaerobic bacterial communities) may also be responsible for changes to $\delta^{18}\text{O}_{\text{diatom}}$ that lead to increasing, but potentially predictable, error in inferred temperatures using this proxy. High resolution, multi-year monitoring can shed light on the complex dynamics affecting $\delta^{18}\text{O}_{\text{diatom}}$ and $\delta^{18}\text{O}_{\text{calcite}}$ and supports the careful use of sedimentary $\delta^{18}\text{O}_{\text{diatom}}$ and $\delta^{18}\text{O}_{\text{calcite}}$ as containing valuable hydroclimatic signals especially at a multi-annual resolution, although there remain substantial challenges to developing a reliable geothermometer on paired $\delta^{18}\text{O}_{\text{diatom}}$ and $\delta^{18}\text{O}_{\text{calcite}}$. In particular, $\delta^{18}\text{O}_{\text{diatom}}$ needs cautious

* Corresponding author.

E-mail address: D.B.Ryves@lboro.ac.uk (D.B. Ryves).

¹ Present address: School of Geography, University of Nottingham, Nottingham NG7 2RD, UK.

² Present address: Department of Earth Sciences and Sprigg Geobiology Centre, University of Adelaide, SA 5005, Australia.

³ Present address: Centre for Ecology and Hydrology, Environment Centre Wales, Deiniol Road, Bangor, Gwynedd LL57 2UW, UK.

interpretation where silica post-mortem secondary alteration is incomplete and diatom preservation is not perfect, and we recommend dissolution be routinely assessed on diatom samples used for isotopic analyses.

1. Introduction

The oxygen isotope composition of diatom silica ($\delta^{18}\text{O}_{\text{diatom}}$) and endogenic calcite ($\delta^{18}\text{O}_{\text{calcite}}$), is controlled by three factors: both the temperature and $\delta^{18}\text{O}$ of the water in which they form, and (potentially) both diagenetic and disequilibrium effects. Individually, $\delta^{18}\text{O}$ of diatom silica or calcite are often used as tracers of past lake water temperature and hydrological balance, an approach that is potentially strengthened when applied together (Lamb et al., 2005; Swann et al., 2010; Dean et al., 2013). Nevertheless, both proxies share the fundamental limitation that they respond to both temperature change and the $\delta^{18}\text{O}$ of lake water ($\delta^{18}\text{O}_{\text{lake}}$) in which they form. Additionally, diagenesis (e.g. dissolution) and non-equilibrium effects may affect the signals themselves (Teranes et al., 1999a; Moschen et al., 2006; Smith et al., 2016). Analysing the two in tandem can explore some of these issues, allowing for an independent temperature prediction (a

geothermometer). Although this has been explored with sedimentary data (Rozanski et al., 2010), no studies, as far as we are aware, have done so in modern environments. Such a geothermometer would have great potential for application in a range of lakes where both diatoms and calcite are preserved in the same sedimentary samples.

Questions remain concerning the degree to which processes occurring during signal acquisition and subsequent alteration can bias the interpretation of $\delta^{18}\text{O}_{\text{diatom}}$ and $\delta^{18}\text{O}_{\text{calcite}}$ as environmental proxies. For $\delta^{18}\text{O}_{\text{diatom}}$, species-specific (vital) offsets during valve silicification have been reported (e.g. Swann et al., 2007), although this is not always the case (Bailey et al., 2014), whereas there is some evidence of post-mortem alteration of the $\delta^{18}\text{O}_{\text{diatom}}$ signal preserved in the frustule, both through diatom dissolution (Smith et al., 2016), and, independent of this, rapid post-mortem dehydroxylation of fresh diatom silica (Dodd and Sharp, 2010; Dodd et al., 2012; Tyler et al., 2017). Under certain conditions, calcite can precipitate out of isotopic equilibrium with

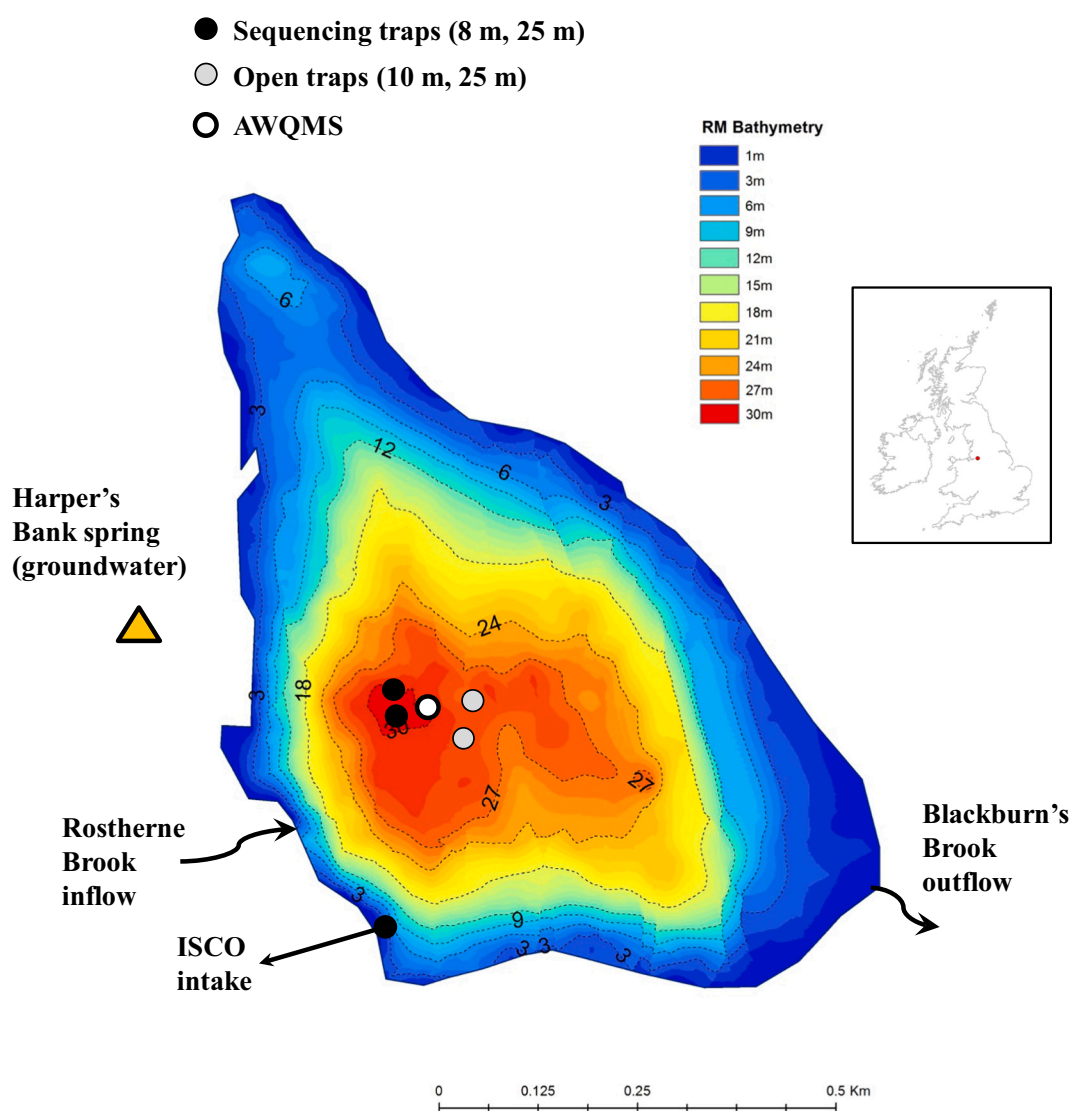


Fig. 1. Location and bathymetric map of Rostherne Mere, Cheshire, UK (adapted from Scott, 2014). AWQMS = Automatic Water Quality Monitoring Station. Harper's Bank spring (orange triangle) was sampled as a groundwater source for the lake. Rostherne Brook (the main inflow) and the single surface outflow (Blackburn's Brook) are indicated. The ISCO automatic water sampler intake (from the littoral of the lake) is also shown.

formation waters (Teranes et al., 1999a), whereas the role of subsequent calcite dissolution on $\delta^{18}\text{O}_{\text{calcite}}$ is unknown.

Despite the uncertainties that plague the interpretation of $\delta^{18}\text{O}_{\text{diatom}}$ and $\delta^{18}\text{O}_{\text{calcite}}$ as palaeoclimatic proxies, only a handful of studies have integrated contemporary seasonal measurements of limnological conditions (such as temperature, pH) and lake $\delta^{18}\text{O}$ composition with direct measurement of the $\delta^{18}\text{O}$ signal of in-situ endogenic calcite or diatom silica (Moschen et al., 2006; Li and Han, 2010; Dean et al., 2015). Here, we combine seasonal limnological monitoring with analyses of $\delta^{18}\text{O}$ in both contemporary diatom silica and calcite soon after their genesis in the water column, and before longer term diagenetic alteration and temporal blurring of the signals as they become incorporated into the sediment archive. This provides the opportunity to examine the production of these signals in more detail, and how they correspond to and capture information about the contemporary lake system, as a means to calibrate the $\delta^{18}\text{O}$ signal from palaeoenvironmental studies of sedimentary records (see Teranes et al., 1999a; Moschen et al., 2006; Dodd et al., 2012).

The purpose of this study was two-fold. Firstly, to assess the correspondence between the surface lake isotope composition and the signal contained within endogenic calcite and planktonic diatoms over two-weekly to seasonal timescales. Secondly, to examine the relationships between physical limnology (e.g. stratification and mixing), hydroclimatology (seasonal change and short-term events, e.g. river flood inputs), and the isotope composition of the hydrological system (rainfall, groundwater, lake water, inflow, outflow), to determine the main drivers of water column isotope variability in a well-characterised lake. In combination, these objectives provide a means to explore the reliability of sedimentary $\delta^{18}\text{O}_{\text{diatom}}$ and $\delta^{18}\text{O}_{\text{calcite}}$ as palaeohydroclimatic (temperature) proxies at seasonal scales in such a system. As a case study, we use a temperate, strongly stratifying, productive lake in the UK (Rostherne Mere, Cheshire) as a natural laboratory in which to explore the isotope systematics manifested in the modern calcite and diatom silica, with high-frequency (two-weekly to monthly) and seasonal sediment traps and water sampling over a two-year period, and generate an isotopic dataset that is unique (as far as we are aware). We also assess the implications of the results for the reliable application of $\delta^{18}\text{O}_{\text{diatom}}$ and $\delta^{18}\text{O}_{\text{calcite}}$ as palaeoenvironmental proxies in their own right, and examine some of the challenges that exist to developing a geothermometer to infer past lake surface temperature from paired $\delta^{18}\text{O}_{\text{diatom}}$ and $\delta^{18}\text{O}_{\text{calcite}}$ data from the same sediment samples.

2. Study site and sampling

2.1. Rostherne Mere

Rostherne Mere (53°20'N, 2°24'W; Fig. 1), one of the Shropshire-Cheshire meres (Reynolds, 1979), is a relatively deep (31 m maximum depth), small (lake area 49 ha), freshwater, monomictic and eutrophic lake. The lake is of glacial origin, and has been deepened by dissolution of underlying salt-bearing strata (Reynolds, 1979) and lies within till, which supplies the lake with bicarbonate ions through inflows and groundwater. The mere is unusually deep for its area (surface area to maximum depth [A_0/Z_{max}] is 0.016), with some topographic protection from westerly winds, and generally stratifies from mid-April to late November or early December (Scott, 2014; Radbourne et al., 2017). Naturally strong monomictic stratification has been exacerbated by eutrophication, especially over the 20th century, when the two catchment sewage treatment works (STWs) were overwhelmed by a growing surrounding population (Carvalho et al., 1995).

Most of the lake's 9 km² catchment area is drained by Rostherne Brook (Fig. 1), the only significant surface inflow, although deep and shallow groundwater must also contribute to the water balance (Carvalho et al., 1995). Lake water outflow is to the east via Blackburn's Brook (Fig. 1). The lake is eutrophic, with a high bicarbonate alkalinity (mean values from 2010 to 12; 1900 $\mu\text{M L}^{-1}$) and high concentrations

of phosphorus (mean TP; $\sim 7 \mu\text{M L}^{-1}$), nitrogen (mean TN; $\sim 87 \mu\text{M L}^{-1}$) and silica (spring maximum $\sim 72 \mu\text{M Si L}^{-1}$). Lake net primary production is high (NEP $\sim 130 \text{ g C m}^{-2} \text{ year}^{-1}$ in 2011–12 with individual algal blooms $> 20 \text{ g m}^{-2}$ dry weight; Reynolds, 1979; Scott, 2014). Planktonic diatoms typically bloom in spring (notably *Asterionella formosa*, *Stephanodiscus neoastraea* and *S. parvus*) and autumn (*Aulacoseira granulata*, *Cyclostephanos dubius* and *C. tholiformis*; Radbourne, 2018), while cyanobacteria (*Microcystis*) dominate in summer (Reynolds, 1978; Livingstone and Reynolds, 1981; Moss et al., 2005; Hargreaves et al., 2013; Radbourne et al., 2017). Under the strong stratification, respiration of the sinking algal crop from the spring and early summer turns the hypolimnion anoxic within only a few weeks (Scott, 2014). Given the lake's large volume relative to surface inflow and outflow, Rostherne Mere has a relatively long water residence time (~ 1.6 years, as calculated from the outflow method; Carvalho, 1993; 2.4 ± 0.25 years using the runoff method; Moss et al., 2005) though more recent data from 2016 suggest it may be < 1 year (Radbourne, 2018). Lake level responds rapidly to increased inflow during periods of high rainfall, and usually falls over summer due to high evaporation. Lake level typically varies by ~ 1 m over an annual cycle.

Rostherne Mere has been monitored (physical, chemical, biological) for over 100 years (e.g. Tattersall and Coward, 1914; Grimshaw and Hudson, 1970; Reynolds, 1978). There was a renewal of scientific interest following the diversion of sewage from the lake in 1991 (e.g. Carvalho et al., 1995; Krivtsov et al., 2001; Moss et al., 2005). The lake currently hosts an on-lake automated water quality and weather monitoring station (AWQMS), as part of the UK Lake Ecological Observatory Network (UKLEON; <http://www.ceh.ac.uk/our-science/projects/uk-lake-ecological-observatory-network-ukleon>), continuing the long-term monitoring of seasonal stratification at Rostherne which has been ongoing since autumn 2005.

2.2. Lake profile temperature data

Thermistors were installed in the lake (at the AWQMS; Fig. 1) and measured temperature continuously at 12 depths (every 2 m) from 0.5 m to ~ 24 m, recording a value every 15 min. These data were averaged to give daily values for each 2 m depth point and processed within Surfer 8 to map lake water isotherms over time. Mixing depth was estimated as the depth of the thermocline, the depth at which the vertical change in temperature was greatest (typically falling by > 1 °C per m), and stratification and overturn periods defined by when the thermocline appeared in spring and disappeared in late autumn/early winter.

2.3. Water sampling

During regular visits to the lake, from February 2010 to May 2012, water samples for oxygen and hydrogen isotope analyses were collected from the centre of the lake at the AWQMS site (Fig. 1) using 30 mL polypropylene bottles. These were rinsed twice with lake water prior to complete filling. Sampling was carried out, on average, every 2–3 weeks throughout the year, except during winter months (January, February) when up to monthly visits were made. On every visit, samples were collected from 0.5 m water depth and the inflow (Rostherne Brook), and less frequently, from 12 m and 24 m water depth using a Ruttner water sampler (1.5 L), as well as the outflow, and groundwater from a spring at Harper's Bank (Fig. 1). Samples from 0.5 m depth were taken to avoid any surface water boundary effects.

An automatic Teledyne-ISCO water sampler was also installed, collecting water from the littoral zone (~ 1 –2 m depth; 10 m from the shore) near to the boathouse (Fig. 1) every 2 weeks during summer 2010, to test if automatic water collection for isotope analyses and on-site storage could be used to reduce the frequency of trips to the lake. Over two periods in summer 2010 (6 and 8 weeks), 750 mL samples

were collected in 1 L bottles to which were added 20 mL of analytic-grade liquid paraffin to prevent evaporation. These samples were stored within the ISCO sampler at ambient temperature and collected at the end of the two periods.

2.4. Sediment trapping

Systematic and high-frequency monitoring of the lake and settling particles began in spring 2010, although some sediment trapping with open traps was carried out prior to this (from autumn 2005; Table 1). Sediment traps were installed in the central pelagic area (~28–30 m water depth, Fig. 1) using both open-tube and fully automatic and programmable rotating-carousel sequencing traps (model Technicap PPS 4/3; Radbourne et al., 2017). The first sequencing trap was installed in May 2010 at 10 m depth (“shallow”), and a second (“deep”) sequencing trap in April 2011 at 25 m water depth. As the thermocline is shallower than 10 m for much of the stratified period, both upper and lower traps integrate the bulk of pelagic diatom silica and calcite production (i.e. summer production) within the lake.

Open-tube traps are composed of an array of 3 or 4 plastic tubes (450 mm length, 72 mm internal diameter) with a trapping ratio (length/diameter) of 6.25. Open-tube traps were set at ~8–10 m (shallow) and 22 m (deep) until May 2010, after which both open-tube traps were set to collect at 22 m. These were emptied after different time periods, from 2 weeks up to ~1 year. Once both shallow and deep sequencing traps were installed in May 2010, the open-tube trapping interval was set to every ~3 (occasionally 4) months. Additionally, open traps (at 8 m and 22 m) were set for various periods starting in autumn 2005 until 2010, allowing some comparative analyses of the isotope composition of calcites and diatom silica prior to the systematic monitoring period.

The sequencing traps (trapping area 0.05 m², trapping ratio 5.2) were programmed to collect seston in 12 × 250 mL polypropylene bottles at ~2-week intervals for 10 months a year (March to December), and monthly in January and February (when productivity was at its lowest). Sequencing traps were reset every ~6 months as dictated by the trapping interval used (~April and September). Sediment trap samples were stored in polypropylene bottles and kept frozen until analysis.

3. Analytical methods and data analysis

3.1. Stable isotope analyses

We use the standard definition for $\delta^{18}\text{O}$, where $\delta^{18}\text{O}_{\text{sample}} = 1000 \times [({}^{18}\text{O}_{\text{sample}}/{}^{16}\text{O}_{\text{sample}} - {}^{18}\text{O}_{\text{standard}}/{}^{16}\text{O}_{\text{standard}}) / ({}^{18}\text{O}_{\text{standard}}/{}^{16}\text{O}_{\text{standard}})]$. Water isotopes ($\delta^{18}\text{O}$, $\delta^2\text{H}$) were analysed in batches at the NERC Stable Isotope Facility, British Geological Survey (BGS). Polypropylene bottles have been tested for secure storage for > 1 year at BGS. Samples were taken directly from the ISCO bottles using a long syringe to sample well below the paraffin layer, but were otherwise analysed according to standard methods. $\delta^{18}\text{O}$ measurements were carried out using the CO₂ equilibration method with an Isoprime 100 mass spectrometer plus Aquaprep device. $\delta^2\text{H}$ measurements were made using an online Cr reduction method with a EuroPyrOH-3110 system coupled to a Micromass Isoprime mass spectrometer. Isotope measurements were normalised against internal standards calibrated against the international standards V-SMOW2 and V-SLAP2. Errors were $\pm 0.05\text{‰}$ for $\delta^{18}\text{O}$ and $\pm 1.0\text{‰}$ for $\delta^2\text{H}$.

Seston samples were freeze dried and subsampled for loss-on-ignition following standard methods (Dean Jr., 1974) to estimate organic content (550 °C for 2 h, error $\pm 2\%$) and carbonate content (925 °C for 4 h, error < 4%). Calcite crystals are known to form endogenically within the upper water column as a result of algal photosynthesis (Livingstone and Reynolds, 1981; Scott, 2014; Radbourne, 2018), in agreement with the calcite saturation index (CSI; Fig. 2). Here, we use

Table 1
Values of $\delta^{18}\text{O}$ for open trap diatom and authigenic calcite samples (relative to both VPDB and VSMOW-SLAP; Coplen, 1995) collected prior to monitoring began in 2010 at Rostherne Mere. Multiple open tubes deployed in the same trap array allow for some estimation of within-sample variability for $\delta^{18}\text{O}_{\text{calcite}}$ values (increasing analytical error slightly).

Open trap sample $\delta^{18}\text{O}$ type	Date in	Date out	No. days	Trap depth (m)	Sample $\delta^{18}\text{O}_{\text{VPDB}}$	Sample $\delta^{18}\text{O}_{\text{VSMOW}}$	Calcite $\delta^{18}\text{O}$ error (tube replicates)
Calcite samples							
Calcite – replicate tube 1	18/11/2005	6/10/2006	322	25	-7.2	+23.50	Range 0.09
Calcite – replicate tube 2	18/11/2005	6/10/2006	322	25	-7.1	+23.59	
Calcite – replicate tube 1	17/11/2006	5/10/2007	322	25	-6.7	+24.04	SD 0.25
Calcite – replicate tube 2	17/11/2006	5/10/2007	322	25	-6.2	+24.56	
Calcite – replicate tube 3	17/11/2006	5/10/2007	322	25	-6.4	+24.34	
Calcite – replicate tube 1	22/11/2007	3/10/2008	316	25	-7.2	+23.55	Range 0.3
Calcite – replicate tube 2	22/11/2007	3/10/2008	316	25	-7.5	+23.24	
Calcite – range within 3 sets of replicates (total 7 samples)			316–322	25			Average error = 0.13
Diatom samples							
Diatom silica	7/10/2005	18/11/2005	42	8		+29.5	
Diatom silica	7/10/2005	18/11/2005	42	25		+31.4	
Diatom silica	14/11/2008	20/11/2009	371	25		+29.7	

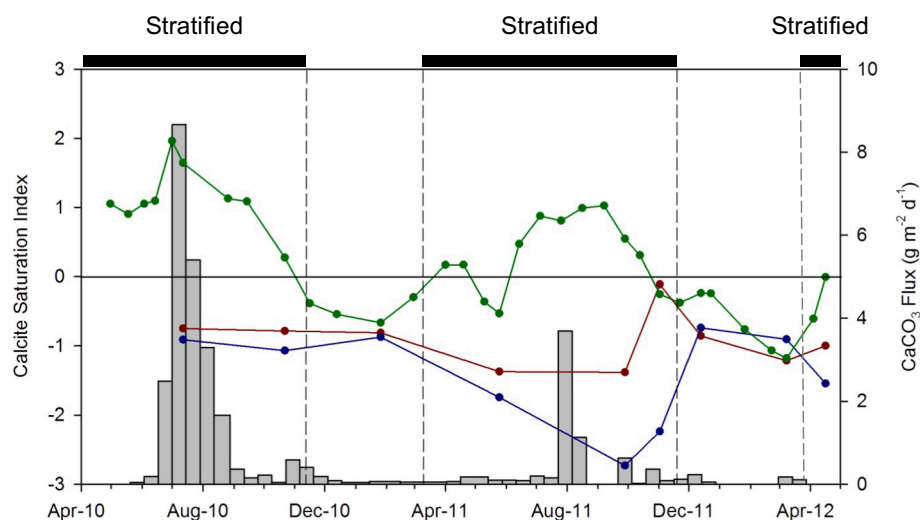


Fig. 2. Calcite saturation index (CSI) and calcite flux at Rostherne Mere, April 2010 – April 2012. Lines (left hand scale) show calcite saturation index for water depths of 0.5 m (green), 12 m (red) and 24 m (blue). Values of CSI > 0 imply supersaturation with respect to CaCO₃ and values < 0 signify CaCO₃ undersaturation. Grey bars (right hand scale) show shallow (10 m) sequencing trap CaCO₃ flux data. The times when the lake was stratified (black bars) are also shown.

the formulation $CSI = pH_m - pH_c$, where pH_m is pH measured in the water and pH_c is pH of the water when in equilibrium with calcite (APHA, 2005; Scott, 2014). Fig. 4 shows that calcite production occurs in spring and summer periods when algal production is high (with algal communities dominated by diatoms in spring and autumn, and cyanobacteria in summer; Radbourne, 2018). At Rostherne Mere, from 2010 to 12, only trap samples collected during the stratified period contained enough material for isotopic analyses of calcite (Table 2, Fig. 2). Identification of trigonal crystals under SEM inspection and yields of CO₂ from isotope analysis (see below) demonstrated that the material collected in the traps was calcium carbonate (calcite).

Samples with high carbonate (> 10% CaCO₃ by dry weight) and sufficient material were selected for bulk oxygen and carbon isotope analyses of carbonates ($\delta^{18}O$, $\delta^{13}C$), with the average ratio of organic to total carbon (OC:TC) in analysed samples of 0.57 ± 0.2 . The samples were immersed in 5% sodium hypochlorite solution (10% chlorox) for 24 h to oxidise the reactive organic material. Samples were then washed three times in distilled water, dried at 40 °C, and ground in an agate mortar and pestle. The isolated material was reacted with anhydrous phosphoric acid in vacuo overnight at 25 °C. The liberated CO₂ was separated from water vapour under vacuum and collected for analysis. Measurements were made on a VG Optima mass spectrometer. Overall analytical reproducibility for these samples is better than 0.1‰ for $\delta^{13}C$ and $\delta^{18}O$ (1SD). Isotope values ($\delta^{13}C$ and $\delta^{18}O$) are reported as per mil (‰) relative to the V-PDB and V-SMOW scales (Tables 1 and 2) using a within-run laboratory standard calibrated against NBS standards (NBS-19 and NBS-28).

Diatom samples for oxygen isotope analyses were purified following the cleaning steps described by Morley et al. (2004), which include oxidation of organic matter with hydrogen peroxide, sieving, differential settling and density separation. Prior to analyses, diatom sample purity was assured by inspection via SEM and by XRF measurements; samples for $\delta^{18}O_{\text{diatom}}$ analyses contained on average ~60 mM Si. $\delta^{18}O_{\text{diatom}}$ was analysed using a step-wise fluorination method (Leng and Sloane, 2008). The outer hydrous layer of the diatom was removed in a pre-fluorination step using a ClF₃ reagent at low (250 °C) temperature. Within this step, a stoichiometric deficiency of reagent removes ~20% of the oxygen, which has been shown to result in values that plateau (Leng and Sloane, 2008). This was followed by a full reaction at high temperature (500 °C) to liberate oxygen that was converted to CO₂ and measured for $\delta^{18}O_{\text{diatom}}$ using a MAT 253 dual-inlet mass spectrometer. All $\delta^{18}O$ values were converted to the V-SMOW scale using the within-run laboratory standard diatomite, BFC_{mod}. In detail, samples are run as CO₂ against the VDPD standard through in-house reference material calibrated through NBS-19, and converted to

V-SMOW using Coplen et al. (1983), then normalised to $\delta^{18}O_{\text{BFC}}$ ($+28.9 \pm 0.3\text{‰}$; $n > 1000$; Chaplignin et al., 2011). For a given number of samples analysed, an additional 20% of standards are run and 10% are replicates. Errors (1SD) for $\delta^{18}O_{\text{diatom}}$ were 0.3‰.

Separate assessments of diatom species composition and assemblage dissolution were made on cleaned trap samples under phase-contrast light microscopy ($\times 1000$) which also revealed when different diatom taxa bloomed (Radbourne et al., 2017; Radbourne, 2018). Dissolution was assessed using the proportion of valves showing no visible signs of dissolution compared to the total number counted, reported as the F index (Ryves et al., 2001; Ryves et al., 2013). F values vary between 0 (all valves partially dissolved) and 1 (all valves pristine).

3.2. Temperature data and isotope calculations

The isotope composition of diatoms and calcite from the traps represent discrete time periods over which they were formed. Average temperatures in the upper water column (where diatoms were growing and calcite was precipitating; Raubitschek et al., 1999) over the period represented by the individual trap samples were calculated using the thermistor data, with averages calculated over the upper 0–4 m and 0–6 m water column (Raubitschek et al., 1999). Endogenic calcite crystals precipitated at the same time as the trap sample in which they were deposited (Fig. 2), but as individual diatom valves might have been formed earlier and stayed in suspension several days before sinking into the traps (see Miklasz and Denny, 2010), temperatures were calculated using a one-week offset. Furthermore, whereas silica precipitation in diatoms is thought to occur during photosynthesis, it may also proceed during dark conditions (Werner, 1977; Martin-Jezequel et al., 2000), so we used both average daytime (0600 to 1800) water temperatures as well as 24 h averages. There are thus two temperatures for each calcite isotope value (integrating over two depths: 0–4 m and 0–6 m), and eight for diatoms (integrating temperatures over two depths, two trapping periods, and daylight/24 h). The differences between these values are small, but for shorter sampling periods (i.e. sequencing trap samples) at certain times of rapid lake temperature change, they may be significant.

Theoretical temperature values derived from $\delta^{18}O_{\text{calcite}}$ and $\delta^{18}O_{\text{diatom}}$ compositions were calculated using the lake surface (0.5 m) $\delta^{18}O$ for that sampling period (no $\delta^{18}O$ gradient was observed in the upper 6 m; Fig. 4) and compared to measured temperatures as above. A number of different fractionation factor-temperature relationships are available in the literature for both $\delta^{18}O_{\text{calcite}}$ (e.g. Kim and O'Neil, 1997; Coplen, 2007) and $\delta^{18}O_{\text{diatom}}$ (see below). The empirically-derived fractionation factor of Kim and O'Neil (1997) has been applied across a

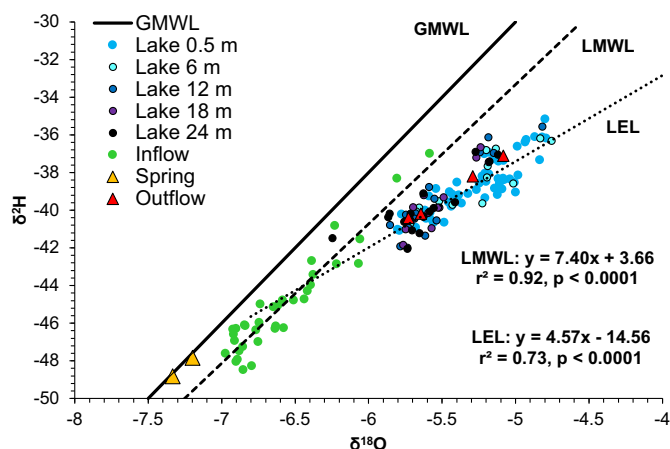


Fig. 3. Correlation of $\delta^{18}\text{O}$ and $\delta^2\text{H}$ for the Rostherne Mere system. Lake water samples are shown by filled circles for 0.5 m, 6 m, 12 m, 18 m and 24 m water depths. Catchment waters are indicated: Rostherne Brook inflow (green circles), Harper's Bank spring groundwater (orange triangles), outflow (red triangles). The GMWL (global meteoric water line), local meteoric water line (LMWL) and local evaporation line (LEL) are plotted (linear regressions between measured $\delta^{18}\text{O}$ and $\delta^2\text{H}$ for the different water types), and regression equations for the LMWL and LEL are given. See Fig. 1 for sampling locations within the lake.

wide range of temperatures, and is the most appropriate model to use here for $\delta^{18}\text{O}_{\text{calcite}}$ (see Eq. (1), Section 5.3.2). In contrast, the spectrum of published silica-water fractionation factors (e.g. Fig. 6b) do not represent true fractionation factors but combinations of different end members representing fresh biogenic silica-water and quartz-water equilibria. Several published fractionation factors were applied to the $\delta^{18}\text{O}_{\text{diatom}}$ data, namely Juillet-Leclerc and Labeurie (1987), Shemesh et al. (1992), Dodd and Sharp (2010) and Moschen et al. (2005). The best fit for $\delta^{18}\text{O}_{\text{diatom}}$ under all possible temperature sets, as defined above, was found using Moschen et al. (2005; Eq. (3), Section 5.3.2), with all other models producing estimates with substantial errors (with $r^2 < 0.6$ for predicted ~ observed temperature for all other models). We appreciate that this does not represent the true silica-water fractionation factor, but we apply this fractionation factor to explore how diagenetic effects impact the temperature signal in the diatom silica host.

4. Results

4.1. The stable isotope composition of the lake- and catchment waters

The $\delta^2\text{H}$ and $\delta^{18}\text{O}$ of the catchment waters (surface and groundwater inflow to the lake) lie along a local meteoric water line (LMWL) (this study). This is offset but parallel to the global meteoric water line (GMWL; Fig. 3), which varies regionally with humidity. In contrast, the lake water isotope composition deviates from the LMWL along a local evaporation line (LEL), due to lake water evaporation in the spring and summer months. As expected, surface and shallow lake waters (< 6 m) show the most enrichment in ^2H and ^{18}O . Evaporative enrichment of the lake water is a function of the relatively long water residence time (~1–2 years), and the strong lake water stratification over the summers which preclude mixing of the evaporated water (high $\delta^2\text{H}$ and $\delta^{18}\text{O}$) with deeper (fresher, lower $\delta^2\text{H}$ and $\delta^{18}\text{O}$) waters for ~8 months of the year.

4.2. Seasonal patterns of stratification and lake water $\delta^{18}\text{O}$

The development of seasonal stratification is typical of warm monomictic lakes, though the lake is stratified longer than most lakes at

~8 months of the year (due to its high relative depth and sheltered position, likely enhanced by high algal productivity in spring absorbing radiation). Stratification at Rostherne usually develops in April, starts to break down in October with complete overturn in late November or early December, with almost all pelagic production occurring while the lake is stratified. In 2011, stratification had established by the end of March following an exceptionally cold winter, when (unusually) the lake completely froze in January and February.

Rostherne Brook $\delta^{18}\text{O}$ values are generally between -7 and -6‰ (probably representing an average shallow water composition of mixed annual rainfall). There are occasional excursions to higher (October 2010, December 2011) or lower values (March 2010) coinciding with significant rainfall events (Fig. 4). The degree to which rainfall amount and $\delta^{18}\text{O}$ values are transmitted into the inflow depends largely on antecedent moisture conditions in the catchment. Greater evapotranspiration in summer across the vegetated catchment reduces the amount of discharge generated from summer rainfall, while in autumn or winter, reduced evapotranspiration and high catchment soil moisture levels from preceding rainfall result in efficient, rapid, and highly variable river runoff. There is no clear systematic rise in river $\delta^{18}\text{O}$ over the summer months in either year, despite the clear summer evaporative signal in the lake, which again suggests the intrusion of shallow groundwater (or the low impact of evaporation rate relative to flow rate in the lotic environment).

In contrast to the inflow stream, patterns of $\delta^{18}\text{O}$ within the lake water column show clear seasonality, reflecting climatic effects as well as stratification and mixing. At the start of the year (January/February) when the lake is mixed, there is no significant differentiation within the 30 m water column in terms of $\delta^{18}\text{O}$ values, which all lie within the analytical uncertainty ($\pm 0.05\text{‰}$). Quickly after stratification is established (~April), however, the upper water column (surface and 6 m depth) becomes isotopically enriched in ^{18}O (i.e. higher $\delta^{18}\text{O}$ values) from seasonal evaporation, while the lower water column (12 m and deeper) maintains $\delta^{18}\text{O}$ values similar to the mixed winter period (Fig. 4). $\delta^{18}\text{O}$ values peak in September 2010 in the surface waters (ca. -5‰), thereafter declining concomitantly with declining water temperatures as the lower lake water column is mixed with the surface waters. In January 2011, when the lake is completely mixed, $\delta^{18}\text{O}$ values throughout the water column (0–24 m) have an average of -5.52‰ ($\pm 0.08\text{‰}$).

This seasonal pattern was repeated in 2011, although the increase in $\delta^{18}\text{O}$ was less rapid, and the peak occurred later in the year (October or November 2011), followed by a rapid $\delta^{18}\text{O}$ decrease into winter (Fig. 4). This appears to reflect the pattern of stratification; in 2011, the maximum water temperature was reached later in the summer, and stratification itself was longer and more stable. Mixing of the lake to 12 m in November 2011 did not have a noticeable effect on $\delta^{18}\text{O}$, perhaps because of increased Rostherne Brook inflow with higher $\delta^{18}\text{O}$ or inter-annual isotopic “memory” of the lake. There is a noticeable trend to increasing $\delta^{18}\text{O}$ over the two study years (winter 2010 values are around -5.5‰ , and -5.2‰ in winter 2011), which is more striking than variations in the inflow. As groundwater $\delta^{18}\text{O}$ does not change, this might result from the cumulative effect of lake water evaporative enrichment over consecutive years, since deep lake water samples also show an increase. Alternatively it might reflect a shift in regional precipitation $\delta^{18}\text{O}$ over this time.

The discharge and hydrochemistry of Rostherne Brook is not clearly reflected in the lake $\delta^{18}\text{O}$ as the lake water volume acts as a buffer (as seen in Fig. 4), although a full characterisation of inflow $\delta^{18}\text{O}$ is difficult without high-frequency monitoring, given the highly variable stream discharge. Individual outflow samples are a good measure of surface water conditions in the lake, and thus an efficient means to sample a lake (in terms of $\delta^{18}\text{O}$) where access to the open water may be an issue. Indeed, at Rostherne Mere, the very good agreement between littoral ISCO and central lake $\delta^{18}\text{O}$ values (Fig. 4e) demonstrates that the upper water column is well mixed spatially across the lake, and thus near-

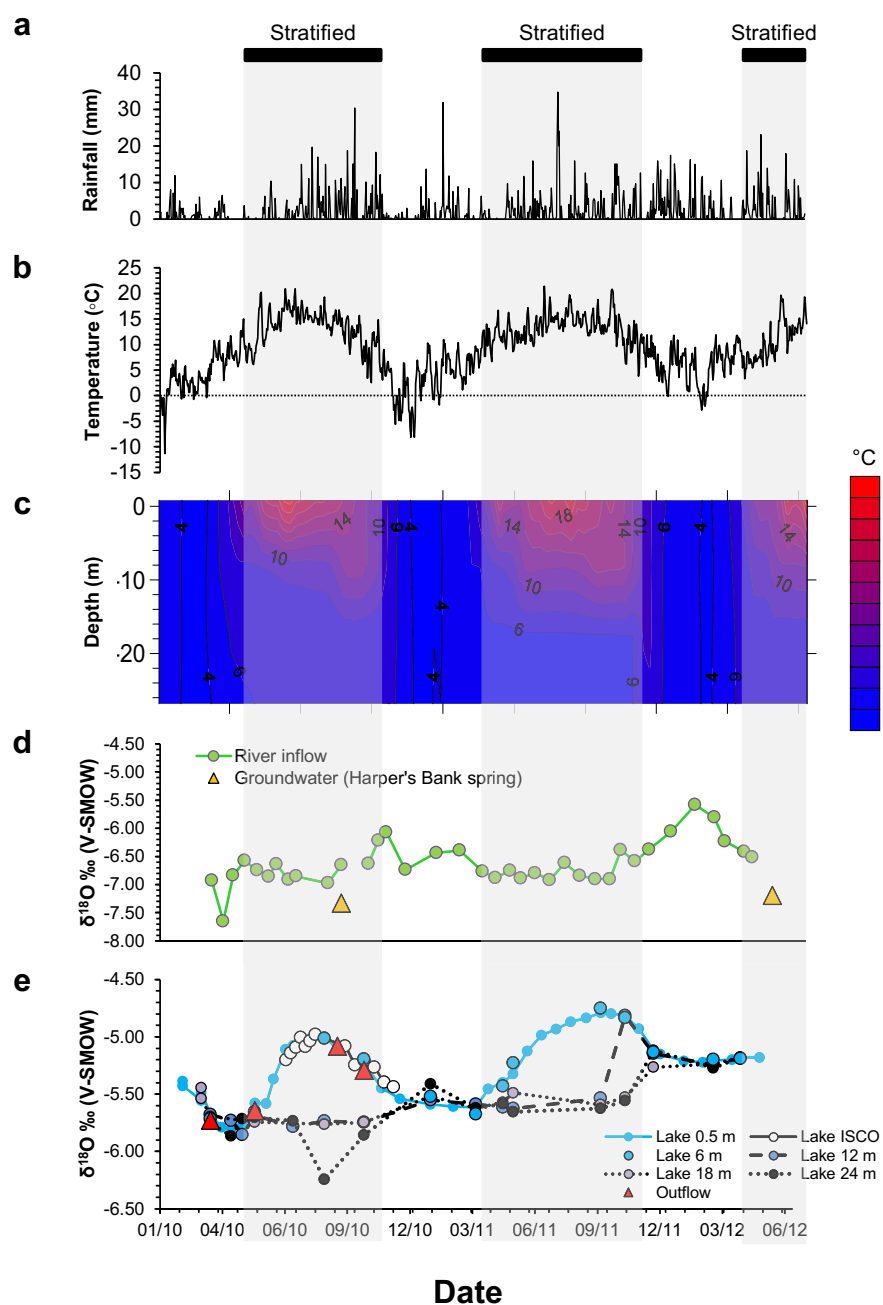


Fig. 4. Time series of regional, catchment and lake data, January 2010 – June 2012. All panels are shown over the common time period indicated under panel e, given in the form month/year from January 1st 2010 to June 30th 2012. Shaded blocks (and black bars above panel a) indicate when the lake was stratified. (a) Daily rainfall measured at Shawbury Meteorological Office station (64 km SW of Rostherne Mere). (b) Air temperature recorded at the on-lake AWQMS (see Fig. 1 for location). (c) Lake isotherms interpolated from the daily average 2 m interval thermistor data. (d) $\delta^{18}\text{O}$ values for Rostherne Brook inflow (green circles) and groundwater (orange triangles; Harper's Bank spring, Fig. 1) (e) $\delta^{18}\text{O}$ values for lake water at different depths (filled circles; 0.5 m, 6 m, 12 m, 18 m and 24 m) and the outflow (red triangles). Littoral samples collected using an automatic ISCO sampler (at ~0.5 m depth; Fig. 1) are shown as empty circles.

littoral sampling for isotope characterisation of upper lake water (i.e. the mixed epilimnion) would be effective. Furthermore, this method of sample collection, and specifically the use of a paraffin layer to stop post-sampling evaporation, can be successfully used for remote sampling and storage on site, even after 2 months within the sampler by the lake at ambient summer temperatures. This approach could improve isotopic monitoring of water bodies that are too remote or otherwise logistically challenging to sample frequently in person.

4.3. Comparison of lake water, $\delta^{18}\text{O}_{\text{calcite}}$ and $\delta^{18}\text{O}_{\text{diatom}}$ of annual and seasonal samples

Calcite $\delta^{18}\text{O}$ (relative to V-PDB and V-SMOW; Tables 1 and 2) and diatom silica $\delta^{18}\text{O}$ (relative to V-SMOW) from sediment traps (collection from 2 weeks, up to ~1 year) are shown in Tables 1–3 and Fig. 5, which also shows trap samples in comparison to surface lake water $\delta^{18}\text{O}$. Table 1 shows the values for samples collected before regular

monitoring of the lake began in 2010 (including replicate tube collections in open trap arrays), while Tables 2 and 3 present data collected during the high-resolution monitoring programme from 2010 to 2012.

Calcite $\delta^{18}\text{O}$ in trap samples recovered from different tubes from the same deep, open traps collecting for a year from 2006, 2007 and 2008 all differ by < 0.5‰ (average difference within three sets of replicate tubes 0.13‰; Table 1), substantially less than the inter-annual variation in average $\delta^{18}\text{O}_{\text{calcite}}$ of about 1‰. These longer-term calcite trap data are consistent (in average and intra-trap range) with the 3-monthly summer values from 2010 and 2011, which are ca. -7.4‰ and -6.7‰ respectively, an inter-annual increase in $\delta^{18}\text{O}$ that parallels changes in surface water $\delta^{18}\text{O}$ from 2011 to 12. These data suggest that multi-year variation in $\delta^{18}\text{O}_{\text{calcite}}$ in the modern system is $\leq 1\%$ (Fig. 5a).

Seasonal or annual samples conceal greater variation on shorter timescales. Through 2010, $\delta^{18}\text{O}_{\text{calcite}}$ exhibits systematically higher values by ~2‰ from June to November (Fig. 5a). This trend is not seen

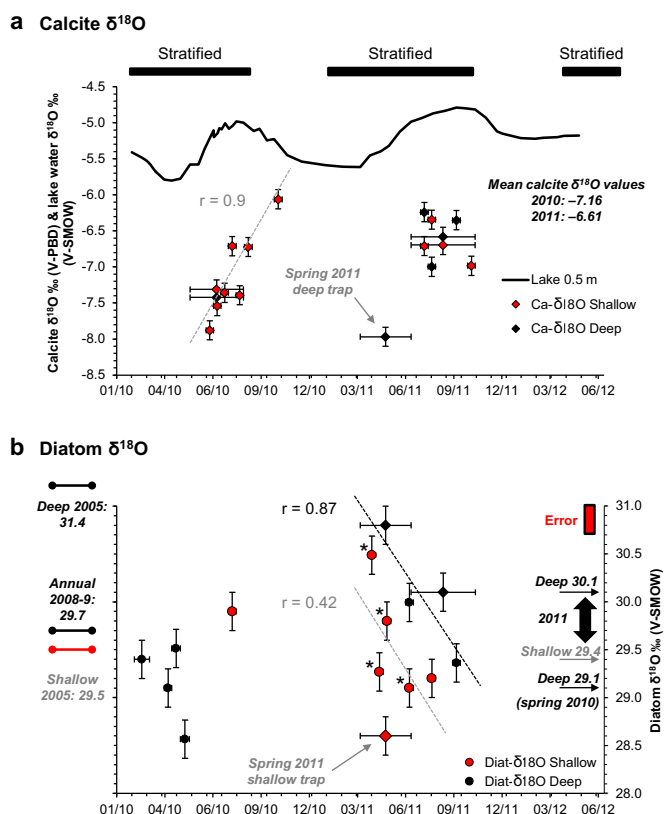


Fig. 5. Time series of lake water $\delta^{18}\text{O}$, calcite $\delta^{18}\text{O}$ and diatom $\delta^{18}\text{O}$ at Rostherne Mere, January 2010 to June 2012. (a) $\delta^{18}\text{O}_{\text{calcite}}$ (deep and shallow traps) and observed lake water $\delta^{18}\text{O}$ (solid line) and (b) $\delta^{18}\text{O}_{\text{diatom}}$ values at Rostherne Mere. Black horizontal bars on (a) indicate periods of lake stratification. Trap type is indicated by symbol: open \blacklozenge and sequencing \bullet , with depth indicated by colour: deep \blacksquare and shallow \blacksquare . Trap samples are plotted at the mid-point for the trap date, with horizontal error bars extending to the first and last dates that each trap was collecting material, while vertical bars are the analytical or replicate errors for $\delta^{18}\text{O}$ values (see Table 1). Linear regressions (with r value) between samples within the same year are included where appropriate (plotted separately for deep and shallow traps for $\delta^{18}\text{O}_{\text{diatom}}$ in 2011). Average annual or seasonal (a) $\delta^{18}\text{O}_{\text{calcite}}$ and (b) $\delta^{18}\text{O}_{\text{diatom}}$ values for 2010 and 2011 are shown to the right; additionally in (b), values of $\delta^{18}\text{O}_{\text{diatom}}$ for trap samples from October–November 2005 and a full year from 2008–9 are shown on the left (all given in Table 1). In (a), one deep trap calcite sample from spring 2011 is highlighted as likely depleted in ^{18}O (RM136; see Table 2 and Section 5.3.1), while in (b) the 2011 spring (3-month) shallow trap $\delta^{18}\text{O}_{\text{diatom}}$ is arrowed (see Section 5.1.2). Red vertical bar to upper right indicates error for $\delta^{18}\text{O}_{\text{diatom}}$ ($\pm 0.3\text{‰}$). In spring 2011, 4 shallow sequencing trap samples indicated with * were collected within the same time period as the shallow open trap.

in 2011, with the exception of an unusually low value in the 3-month open trap in May–June 2011 (Fig. 5a). Values of samples recovered from deep and shallow open traps are within the sampling error (Table 1, Fig. 5a), although this difference is larger ($\sim 0.5\text{‰}$) when compared to the two 14-day trap samples covering the same time period in summer 2011 (though a tendency for higher or lower $\delta^{18}\text{O}$ values is not consistent with depth).

Diatom $\delta^{18}\text{O}$ obtained from a sample integrating over a year from November 2008–November 2009 ($+29.7\text{‰}$; Table 1) is also consistent with values recorded over shorter timescales, especially in 2011 when more samples are available for comparison (Fig. 5b). Over short time periods, $\delta^{18}\text{O}_{\text{diatom}}$ shows considerable variation, for example, between sequential two-weekly samples (e.g. the range among the three deep trap samples from March to May 2010 is $+28.6$ – 29.5‰ , average $+29.1\text{‰}$; Fig. 5b). On a seasonal scale, however, there is a clear trend

in $\delta^{18}\text{O}$ values among 2-weekly and 3-monthly trap samples. This is most strongly evident in the deep-trap samples from 2011, where $\delta^{18}\text{O}_{\text{diatom}}$ is higher in the early growth period (May 2011; ca. $+30.7\text{‰}$) before falling to $+29.2\text{‰}$ by September, with the shallow-trap 2-weekly samples following a similar trend, though with greater variability (Fig. 5b).

In contrast to $\delta^{18}\text{O}_{\text{calcite}}$, there is evidence that there is a depth effect on $\delta^{18}\text{O}_{\text{diatom}}$, with a consistent isotopic enrichment of $^{18}\text{O}_{\text{diatom}}$ in deeper trap samples (Table 3 and Fig. 5b), for both the two-weekly and 2 & 4-month integrated samples (compare October 2005, May 2011 and July 2011). The slope of $^{18}\text{O}_{\text{diatom}}$ isotopic depletion (i.e. lower $\delta^{18}\text{O}_{\text{diatom}}$ values) seen over 2011 is similar between deep and shallow traps but average values differ by $\sim 0.7\text{‰}$ (deep traps: $+30.1\text{‰}$, shallow $+29.4\text{‰}$; Fig. 5b) but up to $+2.2\text{‰}$ between the deep and shallow open trap in spring 2011 (Fig. 5b). Somewhat surprisingly, the shallow trap 3-monthly integrated $\delta^{18}\text{O}_{\text{diatom}}$ value in spring 2011 does not overlap with any of the four two-weekly $\delta^{18}\text{O}_{\text{diatom}}$ collected over the same period at the same depth (arrowed datapoint in Fig. 5b). Both these observations are discussed below.

4.4. Calculated vs measured temperatures from $\delta^{18}\text{O}$ data

Fig. 7 and Tables 2 and 3 show the $\delta^{18}\text{O}$ -inferred temperature against measured lake water temperature for all available $\delta^{18}\text{O}_{\text{calcite}}$ ($n = 21$) and $\delta^{18}\text{O}_{\text{diatom}}$ ($n = 14$) from empirically-derived fractionation relationships using the equations of Kim and O’Neil (1997; $\delta^{18}\text{O}_{\text{calcite}}$) and Moschen et al. (2005; $\delta^{18}\text{O}_{\text{diatom}}$). As too few values from the shallow trap data at Rostherne ($n = 5$, Fig. 6b) are available to calculate a reliable surface water fractionation factor, the fractionation factor of Moschen et al. (2005) was chosen, which is from a similar study (using sub-seasonal trap samples) from a eutrophic, temperate lake (Holzmaar, western Germany) that also stratifies strongly. The comparability of these systems (and hence we argue, processes involved) is supported by the good agreement between the Rostherne and Holzmaar $\delta^{18}\text{O}_{\text{diatom}}$ data (Table 3, Fig. 6b), although there is some inevitable bias introduced. Nonetheless, all models applied for both $\delta^{18}\text{O}_{\text{calcite}}$ and $\delta^{18}\text{O}_{\text{diatom}}$ (for all temperature sets) apparently overestimate lake water temperature, on average by $< 5\text{ °C}$ for $\delta^{18}\text{O}_{\text{calcite}}$ and by $< 1.5\text{ °C}$ for $\delta^{18}\text{O}_{\text{diatom}}$ (for the best fit temperature and time, $\delta^{18}\text{O}_{\text{calcite}}$, average overestimate 6 °C ; $\delta^{18}\text{O}_{\text{diatom}}$ average overestimate 1.85 °C ; Tables 2 and 3), compared to the annual temperature range of $\sim 16\text{ °C}$ in the lake. The data for $\delta^{18}\text{O}_{\text{calcite}}$ imply non-equilibrium calcite precipitation in all cases, with average values around $\sim 1.5\text{‰}$ lower than expected (Fig. 6a). This offset is systematic, however, and we argue that our data do show a temperature effect contained within $\delta^{18}\text{O}_{\text{calcite}}$ and $\delta^{18}\text{O}_{\text{diatom}}$, which we explore further below.

5. Discussion

5.1. Differences between $\delta^{18}\text{O}_{\text{calcite}}$ and $\delta^{18}\text{O}_{\text{diatom}}$ in deep and shallow traps

5.1.1. $\delta^{18}\text{O}_{\text{calcite}}$

Several assumptions are made in interpreting sedimentary lacustrine calcite $\delta^{18}\text{O}$ values (in traps or sediment cores) as a reliable record of ambient water $\delta^{18}\text{O}$ at the time of formation. It is often assumed, but rarely demonstrated, that endogenic calcites precipitate in equilibrium with ambient water (Leng and Marshall, 2004), but more recent work (Coplen, 2007; Daëron et al., 2019) suggests that isotopic equilibrium may only occur during very slow precipitation, which is often not the case in lake systems, especially under eutrophic conditions (Fronval et al., 1995; Teranes et al., 1999a; Teranes et al., 1999b; Bluszcz et al., 2009; Rozanski et al., 2010). Diagenetic processes (e.g. calcite dissolution) have also been shown to impact isotopic compositions, while sediment resuspension can incorporate calcite deposited from previous time periods (and also possibly diagenetically altered by dissolution;

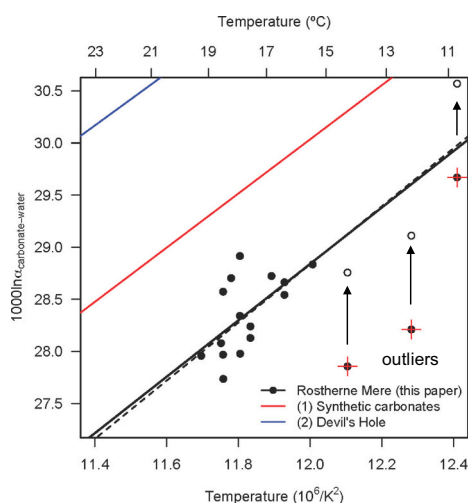
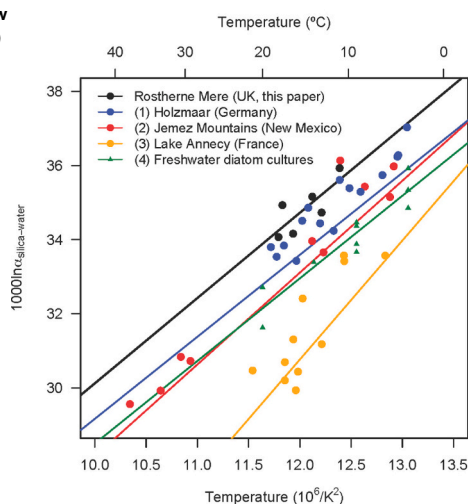
a Calcite $\delta^{18}\text{O}$ **b Diatom $\delta^{18}\text{O}$ (shallow 2-weekly trap samples)**

Fig. 6. Comparison of Rostherne Mere data with previous studies for 18O fractionation against temperature. The α notation (see Section 5.3.2) is used for (a) $\delta^{18}\text{O}_{\text{calcite}}$ and (b) $\delta^{18}\text{O}_{\text{diatom}}$ data from the shallow trap samples, with published fractionation relationships shown for both calcite-water (a) and silica-water (b). In (a), while all Rostherne Mere $\delta^{18}\text{O}_{\text{calcite}}$ samples show non-equilibrium characteristics with ambient lake water, three samples which precipitated during spring or autumn appear especially isotopically light (filled circles with red cross). $\delta^{18}\text{O}_{\text{calcite}}$ values for these three samples have been adjusted (empty circles) by adding +0.9‰ (“adjusted outliers”; see Table 2), as discussed in Section 5.3.1. Regression lines are shown including these three adjusted outliers (solid line) and excluding them (stippled line), with little difference between them suggesting that such an adjustment appears reasonable. The fractionation relationship of Coplen (2007) is derived from stalagmite calcite, while Kim and O’Neil (1997) used experimentally precipitated calcite from a range of temperatures, and are included for comparison with Rostherne Mere sediment trap samples. (b) For $\delta^{18}\text{O}_{\text{diatom}}$, published studies are labelled 1 – 4, from studies where both forming water $\delta^{18}\text{O}$ and temperature were measured. (1) Moschen et al. (2005) from sediment trap samples; (2) Dodd and Sharp (2010) from live diatom communities; (3) Crespin et al. (2010) from live collections of planktonic diatoms; (4) Brandriss et al. (1998) from cultured freshwater diatoms.

Bluszcz et al., 2009). Finally bulk sedimentary calcite may also include biogenically-formed calcite (e.g. produced by green algae such as *Chara* and *Phacotus* spp., or ostracod or mollusc shell; van Hardenbroek et al., 2018), or detrital calcite, washed in from geological deposits within the catchment, with very different isotopic signatures (e.g. Stansell et al., 2017). At Rostherne Mere, sufficient calcite for isotopic analyses was only found in traps from periods when the lake was stratified (during the main periods of endogenic calcite precipitation; Fig. 2; Table 2).

Microscopic examination of trap material, sieve fractions analysed and our understanding of sedimentation dynamics (Radbourne, 2018) allows us to discount the presence of significant quantities of biogenic calcite and catchment (detrital) calcite entering traps during stratification, but non-equilibrium precipitation (see Section 5.3.1) and calcite dissolution (discussed below) may have significant impacts.

There is no evidence for any consistent difference in $\delta^{18}\text{O}_{\text{calcite}}$ between the shallow and deeper traps, despite being separated by some ~15 m (Fig. 5a). Whereas calcite dissolution occurs in the anoxic waters of some lakes (Ohlendorf and Sturm, 2001), trap flux data do not indicate significant loss of precipitated calcite between the two trap depths during the summer (Radbourne et al., 2017; Radbourne, 2018). Following the onset of stratification in early spring and the sedimentation of large algal blooms, the hypolimnion rapidly becomes anoxic from the lake floor and is deoxygenated within ~1 month (Scott, 2014). The calcite saturation index (CSI) at Rostherne from 2010 to 12 (Fig. 2; Scott, 2014) reveals that both deep and shallow traps sit in waters undersaturated with respect to calcite for much of the year (typically CSI ~ -1 in summer at 10 m depth, and between -1 and -2 at 24 m). Calcite dissolution is expected to lead to an enrichment of ^{18}O (Bluszcz et al., 2009) as ^{16}O is preferentially lost from the calcite matrix during dissolution. Our data suggest that any calcite dissolution occurring at Rostherne Mere during the sampling period did not impact $\delta^{18}\text{O}_{\text{calcite}}$, which are within the range of replicate open-tube traps at the same depth (in 2006–7; Table 1). If resuspension of calcite has occurred, the similarity of $\delta^{18}\text{O}$ values between deep and shallow traps implies this has not had any noticeable effect on trap calcite $\delta^{18}\text{O}$ (which also supports evidence that calcite is being formed in the same zone, i.e. the epilimnion).

5.1.2. $\delta^{18}\text{O}_{\text{diatom}}$

Diatom $\delta^{18}\text{O}$ in 2011 differs significantly between deep (25 m) and shallow (10 m) traps, by between 0.7 and 2‰, which is beyond analytical error (Fig. 5b). Earlier work from monthly sediment trap studies in Lake Holzmaar, Germany (Moschen et al., 2006), also showed that $\delta^{18}\text{O}_{\text{diatom}}$ values systematically increase by 2.5‰ between the shallow trap (7 m), deeper trap (16 m), and lake floor (20 m), which was linked to resuspension of $^{18}\text{O}_{\text{diatom}}$ -enriched surface sediment contaminating the traps. More recently, studies of short sediment cores from a shallow freshwater pond in New Mexico revealed that the $\delta^{18}\text{O}_{\text{diatom}}$ signal changes rapidly after the death of the cell during initial maturation, becoming enriched in ^{18}O (more positive $\delta^{18}\text{O}$) within months after sedimentation (Dodd et al., 2012). In contrast to the calcite data, resuspension of such ^{18}O -enriched diatom silica may affect the Rostherne samples, as there is an offset (~1‰) between deep and shallow traps, similar to that found in Lake Holzmaar (Fig. 5b).

At Rostherne, the deeper trap did consistently collect slightly more material (organic, carbonate and mineral matter) than the shallow trap in summer 2011 (Radbourne et al., 2017), implying there was some sediment resuspension and focussing of previously sedimented material from shallower sediments lying above the thermocline, although most resuspension occurs during winter mixing periods. Whereas surface sediments were not analysed directly within this study, other studies have shown that surface sediment $\delta^{18}\text{O}_{\text{diatom}}$ values are higher relative to fresh diatom silica or seston (Moschen et al., 2006), a result of post-mortem silica dehydroxylation (condensation) processes (Dodd et al., 2012; Dodd et al., 2017; Tyler et al., 2017). Alternatively, initial dissolution of fresh, reactive outer silica layers enriched in ^{18}O may lead to higher $\delta^{18}\text{O}$ of the residual silica, as has been observed in experimental phytolith dissolution (Prentice and Webb, 2016). However, in this study, samples from most deeper trap samples analysed for $\delta^{18}\text{O}_{\text{diatom}}$ are no more dissolved than shallow trap assemblages (see Table 3).

Evidence for the alteration of $\delta^{18}\text{O}_{\text{diatom}}$ values on the timescale of months, as proposed by Dodd et al. (2012) who found significant increase in $\delta^{18}\text{O}_{\text{diatom}}$ within 6 months of diatom death, is provided by comparing material from the shallow open and sequencing traps for

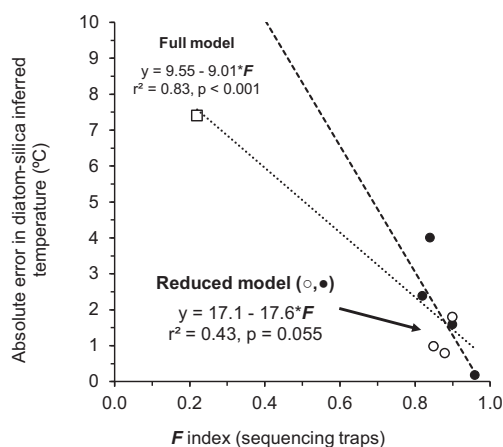


Fig. 7. Relationship between sample diatom dissolution index and absolute error in predicted temperature from $\delta^{18}\text{O}_{\text{diatom}}$. Diatom dissolution is assessed on sample assemblages using the F index (Ryves et al., 2001), with values varying between 1 (all valves pristine) to 0 (all valves visibly dissolved) when counted during routine light microscope analysis. Model error ($^{\circ}\text{C}$) for all sequencing trap samples (both shallow and deep traps) is calculated as the absolute difference between predicted and observed temperature ($|T_{\text{pred}} - T_{\text{obs}}|$) from the best fit model of Moschen et al. (2005; Table 3). Diatom samples that produced overestimates of temperature are denoted by empty symbols (\circ , \square), and those underestimating inferred temperature are filled symbols (\bullet). Even if the sample with the largest error (denoted \square , $\sim 7^{\circ}\text{C}$ overestimate, with F index ~ 0.2) is excluded (“Reduced model”), there is a clear association between model error and dissolution index ($n = 7$, $p = 0.055$), with error tending to increase as the assemblage becomes more dissolved. Under both models, the absolute error (y) is very close to a linear function of $y = a(1-F)$, with a ~ 17 under the reduced model and ~ 9 under the full model (implying very little apparent error for a perfectly preserved diatom assemblage with $F \sim 1$).

spring 2011 (Fig. 5b). The four sequencing trap samples from April to July 2011 (asterisked on Fig. 5b) have $\delta^{18}\text{O}_{\text{diatom}}$ values that are, on average, 1‰ higher than the 3-monthly shallow trap samples covering the same period (Fig. 5b), exceeding analytical error ($\pm 0.3\text{‰}$). There is a substantial overlap in $\delta^{18}\text{O}_{\text{diatom}}$ data from these four 2-weekly traps during the 3-monthly open-trap period (8 of the 12 weeks have 2-weekly $\delta^{18}\text{O}_{\text{diatom}}$ values). Measured diatom biovolume flux ($\sim 10^8 \mu\text{m}^3 \text{cm}^{-2} \text{day}^{-1}$) during this 8-week period dominates total diatom flux into the 3-monthly trap. The difference between 3-monthly and two-weekly $\delta^{18}\text{O}_{\text{diatom}}$ cannot, therefore, plausibly be explained by any flux of extremely low $\delta^{18}\text{O}$ diatom silica in the other 4 weeks (nor do the temperature data support the kind of excursion needed to deliver such low $\delta^{18}\text{O}$ silica to the traps; Fig. 4b). Similarly, resuspension would also affect both trap types equally, as they are located in the same central part of the lake at the same depth. Whereas there is a trend to better preservation over time within the sequencing trap samples (from $F \sim 0.82$ to 0.90; Table 3), early dissolution as the main mechanism of enrichment (Prentice and Webb, 2016) seems less likely as the sample with the lowest $\delta^{18}\text{O}$ (an open trap sample) is also the most dissolved ($F = 0.77$). Sampling logistics may explain this difference, as the early sequencing trap samples (from April 2011) had longer to mature in situ compared to the open trap sample, which was removed from the lake after 3 months in June 2011 and frozen until analysis (with most diatom silica likely in the trap for < 2 months). In contrast, the sequencing trap samples remained in the lake within the carousel until the trap was reset in September 2011, thus the earlier samples had more time to alter (~ 5 months for the April 2011 sample), in agreement with findings from Dodd et al. (2012). Alterations in $\delta^{18}\text{O}_{\text{diatom}}$ through dissolution may partly explain the resultant error in inferred temperature from samples of this trap type (see Fig. 7, discussed in Section 5.2 below).

This alteration or maturation has been linked to dehydroxylation associated with the selective loss of isotopically-light silanol groups ($\text{Si-}^{16}\text{OH}$) (Schmidt et al., 2001; Moschen et al., 2006; Dodd et al., 2017), which in turn should lead to the entrainment of exchangeable, silanol-derived O within the Si-O-Si matrix (Tyler et al., 2017). However, this was not observed by Dodd et al. (2012), who instead suggest that silaffin decomposition (perhaps by anaerobic bacteria) is key. It may therefore be that anoxic conditions and the presence of anaerobic bacteria (as in the hypolimnia of productive lakes or within surface sediments) after the death of the diatom cell initiates this rapid maturation and enrichment. Differences in ambient pH between the shallow and deep traps may alter silica dissolution-reprecipitation kinetics, although at Rostherne Mere, the maximum difference between pH at 10 m and 25 m is 1.2 pH units (in late summer 2011), and generally < 1 pH unit (typically pH ~ 7.6 at 10 m and pH 6.8–7 at 25 m; Scott, 2014). The activity or metabolites of anaerobic bacteria may buffer the system, compared to one where dissolution processes are dominant, or the anaerobic conditions may affect dehydroxylation kinetics of silica through effects on -OH groups. Recent research has suggested that such maturation processes at temperatures typically found in aquatic sediments alter diatom $\delta^{18}\text{O}$ values over long ($\sim 10^4$ – 10^6 years) timescales rather than months (Dodd et al., 2017). Further experimental work is needed to explore this issue further, but our current dataset cannot address this issue, which is beyond the scope of the present study.

The apparent lack of an enrichment effect in the deep-trap samples from spring 2010 (Fig. 5b) supports the conjecture that anaerobic conditions play a role in diatom silica oxygen isotope dynamics. These samples were in oxic water before or during early stratification, and were removed from the lake every 2 weeks for processing, which may have prevented this rapid maturation (Dodd et al., 2012). Regardless of the mechanism, as Moschen et al. (2006) argued, simple isotope exchange with ambient waters of the hypolimnion is not the most logical explanation for the enrichment, since deep water $\delta^{18}\text{O}$ values during the stratified period (when diatoms are growing) are always lower than those in the epilimnion (Fig. 4e). Nevertheless, any consideration of secondary isotope exchange should take into account both the rate and total amount of oxygen exchange as well as the silica-water isotope fractionation during that process, both of which are likely to be temperature dependent. It is possible, for example, that at low temperatures (such as at the bottom of oceans and in the hypolimnia of stratified lakes), the rate of secondary alteration is low, meaning that the time required for alteration is much longer than in warmer conditions. In contrast, mineral-water oxygen isotope fractionation is usually inversely correlated to temperature, such that slow alteration at low temperatures might impart a larger effect on the isotope composition of modified silica. More work is needed to quantify these processes using a combination of structural and isotope analyses.

5.2. The role of diatom dissolution and species composition on $\delta^{18}\text{O}_{\text{diatom}}$ values

At Rostherne Mere, there are distinct changes in diatom preservation (i.e. dissolution) within the trap samples, which may impact $\delta^{18}\text{O}_{\text{diatom}}$ values. Diatom assemblages become more dissolved over time through spring and summer 2011 (F in spring for all traps was ~ 0.80 , dropping to 0.22 in September in the deep traps; Table 3), and are more dissolved in the deep traps (mean $F \sim 0.62$) than in the shallow traps (mean $F \sim 0.86$). Over the same period, $\delta^{18}\text{O}_{\text{diatom}}$ decreases (Fig. 5b), suggesting that the experimental diatom dissolution results of Smith et al. (2016) for slight, but significant, depletion (lower $\delta^{18}\text{O}_{\text{diatom}}$ values) during dissolution hold true for fresh diatom silica as well, although dissolution is clearly not the only, or dominant, driver. The deeper trap silica has a higher $\delta^{18}\text{O}_{\text{diatom}}$ compared to the shallower trap, whereas the opposite would be expected if dissolution dominated $\delta^{18}\text{O}_{\text{diatom}}$ (Fig. 5b; see below), although as discussed above

in Section 5.1.2, resuspension of older sedimented material (which is likely more dissolved) probably drives this signal.

The effect of silica dissolution on $\delta^{18}\text{O}_{\text{diatom}}$ remains controversial, as the few studies that have examined this directly report conflicting results. Experimental diatom dissolution studies have yielded all possible outcomes in $\delta^{18}\text{O}_{\text{diatom}}$ values with increasing dissolution: no change (Schmidt et al., 2001), strong enrichment (by up to +7%; Moschen et al., 2006) and more limited, but still significant, depletion (by up to -1.3%; Smith et al., 2016). Work on phytoliths has shown an initial increase in $\delta^{18}\text{O}$ during dissolution followed by a reduction (to original or lower values; Prentice and Webb, 2016), but the differences between the materials used (diatoms, phytoliths), sample age and amount of dissolution in these experiments make direct comparisons problematic. Smith et al. (2016) used geologically aged diatom samples $\sim 10^5$ – $> 10^6$ years in age, and all appreciably dissolved, whereas Moschen et al. (2006) only found significant change (enrichment) on fresh, cultured diatoms (with no change in samples aged from ~ 5000 years or 2.4 M year). Schmidt et al. (2001) dissolved fresh marine plankton, cultured diatoms and sediment trap material but found no change in $\delta^{18}\text{O}$ after up to 31% of silica loss (intriguingly, a diatom plankton assemblage was depleted in $^{18}\text{O}_{\text{diatom}}$ beyond analytical error despite losing only 2.4% of its silica). Substantial silica loss can occur before this is revealed by routine assessment under light microscopy. In dissolution experiments on mixed assemblages of freshly collected lacustrine diatoms, Ryves et al. (2001) found that even visually well-preserved assemblages (F index values ~ 0.7) could have lost substantial diatom silica ($\sim 30\%$). During such early dissolution, diatom silica may undergo internal reorganisation of the silica structure through accelerated maturation.

Our dataset cannot be used to determine if dissolution imparts a consistent enrichment or depletion of $^{18}\text{O}_{\text{diatom}}$ in samples, as other factors (e.g. variations in surface water $\delta^{18}\text{O}$ and temperature of water) also vary. However, within the sequencing trap samples, there is some evidence that dissolution leads to greater absolute error in inferred temperatures from diatom-silica data (Fig. 7). The relationship suggests a linear dependence of the error on assemblage dissolution (i.e., $1 - F$), and essentially disappears when sample preservation is excellent ($F \approx 1$; Fig. 7). We suggest this may be related to conditions that are fostered within this type of trap, where seston samples are isolated from the surrounding ambient lake water once the sample is collected, and anoxia and associated bacterial communities can rapidly develop. Given widespread diatom dissolution observed in contemporary marine, freshwater and saline systems and their sedimentary archives (e.g. Shemesh et al., 1989; Bidle and Azam, 1999; Ryves et al., 2003, 2006; Ryves et al., 2013) and the conflicting observations from experimental diatom dissolution work from Moschen et al. (2006), Schmidt et al. (2001) and Smith et al. (2016), and our own preliminary findings (Fig. 7), this is an area that clearly merits more thorough experimental investigation. We recommend this be carried out on a range of fresh material covering key assemblages commonly used for palaeoenvironmental inference in marine and freshwater systems. Given the potential impact of dissolution on $\delta^{18}\text{O}_{\text{diatom}}$ -derived proxies suggested by our data (Fig. 7), we further recommend routine assessment of diatom dissolution in samples in the context of $\delta^{18}\text{O}_{\text{diatom}}$, especially where preservation and species composition change.

There is a complete turnover of planktonic diatom species during a typical seasonal succession at Rostherne Mere (Radbourne, 2018), though given the relatively consistent silica-water isotope fractionation relationships published (Moschen et al., 2005; Tyler et al., 2008; Chaplignin et al., 2012; Bailey et al., 2014; Fig. 6b), major species effects seem unlikely. There was insufficient material to carry out rigorous testing of the effect of diatom species or size in the present study.

5.3. Prospects and problems of using $\delta^{18}\text{O}_{\text{calcite}}$ and $\delta^{18}\text{O}_{\text{diatom}}$ for temperature inference

5.3.1. Inter-annual variability and non-equilibrium behaviour of calcite

The results of this study show that patterns within the isotope data for both $\delta^{18}\text{O}_{\text{diatom}}$ and $\delta^{18}\text{O}_{\text{calcite}}$ vary considerably from year to year, and that different drivers may dominate the signal within a mineral host in different years. The expected strong seasonal (i.e. temperature) effect is only seen in the calcite $\delta^{18}\text{O}$ series in 2010 and is not observed in 2011 (Fig. 5a), while the opposite is true for the diatom $\delta^{18}\text{O}$ data (although data are sparse in 2010 for diatom $\delta^{18}\text{O}$). This inter-annual variability highlights potential problems with developing a paired isotope approach for palaeoclimatic inference, as an annual temperature signal may not be consistently recorded in isotopic sedimentary proxies. Instead, in any given year, $\delta^{18}\text{O}$ data may be driven by factors with little or only an indirect relationship to climate, such as stratification pattern or changing nutrient status (e.g. affecting non-equilibrium precipitation dynamics of calcite $\delta^{18}\text{O}$ or seasonality of diatom production), where there may also be a mismatch in timing of the generation of the isotopic signal between proxies (i.e. different production periods of endogenic calcite from diatom silica). Our results suggest that sediment samples that integrate several years may give the most reliable isotopic climate signal, as high-resolution (and especially annual records, such as varves) may have any direct temperature signal overprinted by limnological or chemical processes operating in a given year.

Our results also imply that calcite collected in traps did not precipitate under equilibrium conditions (Fig. 6a). This has been observed in calcites from other eutrophic lakes over seasonal (Sacrower See, Germany; Bluszcz et al., 2009; Baldeggersee, Switzerland; Teranes et al., 1999a) and longer term datasets (Lake Arresø, Denmark; Fronval et al., 1995), as well as in systems recovering from eutrophication (Lake Gościąg, Poland; Rozanski et al., 2010), and is well-known in Chara-precipitated carbonates, for example (Leng and Marshall, 2004). In all these cases, rapid precipitation of calcite related to intense algal photosynthesis resulted in calcite $\delta^{18}\text{O}$ values that were isotopically lighter, from kinetic fractionation effects, often associated with calcite supersaturation in the epilimnion and the production of larger calcite crystals (e.g. Baldeggersee, Lake Gościąg). In the case of Lake Arresø and Baldeggersee, this was consistently observed from sediment samples spanning several decades as the lakes underwent eutrophication (Fronval et al., 1995; Teranes et al., 1999b), whereas in contemporary sediment trap studies from Baldeggersee and Sacrower See (Teranes et al., 1999a; Bluszcz et al., 2009), disequilibrium fractionation in calcites from late spring samples (which dominated annual production) was most obvious. Daëron et al. (2019) suggest that the majority of calcites worldwide, including biogenic carbonates, precipitate out of equilibrium, whereas in a modelling study, Watkins et al. (2014) argue that the effect of mineral growth rate on calcite-water oxygen isotope fractionation is subtly dependent on both pH and temperature. Nevertheless, despite the prevalence of non-equilibrium isotope fractionation, the consistent slope of the temperature effect on calcite-water isotope fractionation between calibration studies suggests that it is actually the intercept of that relationship which varies to the greatest extent (Daëron et al., 2019). Our data from Rostherne Mere support this interpretation, since the slope of the regression in Fig. 6a (with or without the three adjusted points; see below) is parallel to that from Kim and O'Neil (1997) and Coplen (2007) derived from synthetic and stalagmite carbonates respectively, albeit with larger intercept offsets. This apparently systematic offset would then imply that $\delta^{18}\text{O}_{\text{calcite}}$ retains quantitative potential to infer past temperature and hydrological change.

Beyond the general systematic offset of lower $\delta^{18}\text{O}_{\text{calcite}}$ than would be predicted for equilibrium conditions, there also appear to be specific calcite samples that are especially isotopically light (Fig. 6a). A detailed study of seasonal calcite deposition within sediment traps and varves in

Table 2
 Measured $\delta^{18}\text{O}$ for authigenic calcite trap samples from shallow and deep traps, arranged by collection length and then chronologically, from 2010 to 2011 (relative to both VPDB and VSMOW-SLAP; Coplen, 1995). Measured lake surface $\delta^{18}\text{O}$ and inferred temperatures are shown. Inferred temperatures use the equation of Kim and O'Neil (1997) that gave the best fit to a range of measured temperatures, including two depth intervals (upper 0–4 m and 0–6 m of the lake). For three calcite samples, measured $\delta^{18}\text{O}$ was adjusted (*adj.*) for depletion under rapid calcite precipitation (e.g. Teranes et al., 1999a). See Sections 4.4 and 5.3 for further discussion.

Sample code	Trap depth (m)	Trap type	Date in	Date out	No. days	Sample $\delta^{18}\text{O}_{\text{VPDB}}$ (vs PDB)	Sample $\delta^{18}\text{O}_{\text{VSMOW}}$ (vs VSMOW-SLAP)	Lake surface $\delta^{18}\text{O}$	Inf. temp (°C)	Best fit obs. temp (°C)
Calcite $\delta^{18}\text{O}$										
RM67	8	Open	18/05/2010	26/08/2010	100	-7.42	+23.27	0.5 m	Kim and O'Neil (1997)	0–4 m
RM138	8	Open	05/07/2011	02/11/2011	120	-6.58	+24.13	-5.17	24.5	17.55
RM75	10	Sequencing	01/07/2010	15/07/2010	14	-7.54	+23.15	-4.86	21.9	16.39
RM76	10	Sequencing	15/07/2010	29/07/2010	14	-7.36	+23.33	-5.12	25.4	19.25
RM77	10	Sequencing	29/07/2010	12/08/2010	14	-6.71	+24.00	-5.06	24.7	18.56
RM78	10	Sequencing	12/08/2010	26/08/2010	14	-7.39	+23.30	-5.03	21.7	18.21
RM79	10	Sequencing	28/08/2010	11/09/2010	14	-6.72	+23.99	-4.99	25.3	17.90
RM83	10	Sequencing	23/10/2010	06/11/2010	14	-6.06	+25.60	-5.06	21.6	16.83
RM83 (<i>adj.</i>)	10	Sequencing	23/10/2010	06/11/2010	14	-5.16	+24.67	-5.34	17.1	10.72
RM99	10	Sequencing	23/07/2011	06/08/2011	14	-6.71	+24.00	-4.90	22.4	18.49
RM100	10	Sequencing	06/08/2011	20/08/2011	14	-6.34	+24.38	-4.87	20.7	17.91
RM107	10	Sequencing	23/07/2011	06/08/2011	14	-7.34	+23.35	-4.93	25.3	18.49
RM123	10	Sequencing	21/09/2011	05/10/2011	14	-6.35	+24.37	-4.80	21.1	15.44
RM66	25	Open	18/05/2010	26/08/2010	100	-7.31	+23.38	-5.17	24.0	17.55
RM136	22	Open	01/04/2011	05/07/2011	95	-7.97	+23.63	-5.45	25.8	14.28
RM136 (<i>adj.</i>)	22	Open	01/04/2011	05/07/2011	95	-7.07	+22.70	-5.45	21.4	14.28
RM137	25	Open	05/07/2011	02/11/2011	120	-6.70	+24.02	-4.86	22.5	16.39
RM74	22	Sequencing	17/06/2010	01/07/2010	14	-7.88	+22.80	-5.24	26.4	18.48
RM108	25	Sequencing	06/08/2011	20/08/2011	14	-7.00	+23.71	-4.96	23.5	17.91
RM113	25	Sequencing	19/10/2011	02/11/2011	14	-6.98	+24.65	-4.81	24.1	12.19
RM113 (<i>adj.</i>)	25	Sequencing	19/10/2011	02/11/2011	14	-6.08	+23.72	-4.81	19.8	12.19

Table 3
Measured $\delta^{18}\text{O}$ for diatom samples from shallow and deep traps, arranged by collection length and then chronologically, from 2010–2011. Measured lake surface $\delta^{18}\text{O}$ and inferred temperatures are shown, with assemblage F index, assessing dissolution of diatom valves (Ryves et al., 2006). The best fit of inferred (Inf.) to observed (Obs.) temperatures using the equation from Moschen et al. (2005) was for the average observed temperature offset (earlier) by 1 week to the trapping period (time period T2), measured during daylight hours (0600–1800) from the upper 0–6 m of the water column. See Sections 4.4 and 5.3 for further discussion.

Sample code	Trap depth (m)	Trap type	Date in	Date out	No. days	Sample $\delta^{18}\text{O}$	Lake surface $\delta^{18}\text{O}$	Inf. temp (°C)	Best fit obs. temp (°C)	F index
Diatom $\delta^{18}\text{O}$										
RM-BSI135	8	Open	01/04/2011	05/07/2011	95	vs VSMOW +28.6	0.5 m at T2 -5.32	Moschen et al. (2005); T2 18.5	0–6 m, T2, 0600–1800 12.90	0.87
RM-BSI77	10	Sequencing	29/07/2010	12/08/2010	14	+29.9	-5.03	13.6	17.60	0.84
RM-BSI92	10	Sequencing	16/04/2011	30/04/2011	14	+30.5	-5.43	8.6	10.97	0.82
RM-BSI93	10	Sequencing	30/04/2011	14/05/2011	14	+29.3	-5.43	14.8	13.01	0.90
RM-BSI94	10	Sequencing	14/05/2011	28/05/2011	14	+29.8	-5.36	12.5	14.08	0.90
RM-BSI97	10	Sequencing	25/06/2011	09/07/2011	14	+29.1	-5.06	17.3	16.33	0.85
RM-BSI100	10	Sequencing	06/08/2011	20/08/2011	14	+29.2	-4.87	17.9	18.07	0.96
RM-BSI136	22	Open	01/04/2011	05/07/2011	95	+30.8	-5.32	12.4	12.90	0.82
RM-BSI138	22	Open	05/07/2011	02/11/2011	120	+30.1	-4.86	18.6	16.45	0.55
RM-BSI54	24	Open	03/02/2010	03/03/2010	28	+29.4	-5.46	14.0	3.50	0.92
RM-BSI61	22	Open	31/03/2010	14/04/2010	14	+29.1	-5.80	13.8	6.56	0.90
RM-BSI62	22	Open	14/04/2010	30/04/2010	16	+29.5	-5.79	11.7	9.04	0.85
RM-BSI64	22	Open	30/04/2010	17/05/2010	17	+28.6	-5.68	16.7	10.70	0.88
RM-BSI105	25	Sequencing	25/06/2011	09/07/2011	14	+30.0	-4.99	18.3	17.52	0.88
RM-BSI123	25	Sequencing	21/09/2011	05/10/2011	14	+29.4	-4.80	22.6	15.20	0.22

a similarly productive, eutrophic, monomictic lake (Baldeggersee, Switzerland) revealed that rapid precipitation in spring (and to a lesser extent, autumn) resulted in the formation of larger calcite crystals which had isotopically lighter signatures (of ca. -0.7%) compared to theoretical values, possibly due to isotopic disequilibrium through CO_2 hydration and/or hydroxylation (Teranes et al., 1999a). Consequently, at Baldeggersee, the later summer/autumn calcite deposition (darker varve) captured a reliable signal of ambient lake water temperature, rather than the lighter, spring band (Teranes et al., 1999b). Similar results were reported in a comparable hard-water eutrophic Swiss lake (Sopensee), where spring calcite had lower $\delta^{18}\text{O}$ values by $\sim 1.1\%$ (values in Teranes et al., 1999a). This depletion occurred when ambient surface carbonate concentration in the lakes crossed a threshold of between 25 and 50 μM CO_3^{2-} , linked to intense algal blooms and photosynthetic activity, reducing $p\text{CO}_2$, increasing calcite saturation state and promoting calcite precipitation. This was hypothesised to be important in similar hard-water, eutrophic lakes (Teranes et al., 1999a) although it has been observed in calcites in other lacustrine settings (Fronval et al., 1995; Hodell et al., 1998; Bluszcz et al., 2009; Rozanski et al., 2010) and in stalagmites (Coplen, 2007).

Rostherne Mere may behave in a similar way, as measured $[\text{CO}_3^{2-}]$ exceeded 25 μM during spring and autumn during 2010 and 2011 (Scott, 2014) and annual TP concentrations remain over 6.5 μM L^{-1} (Scott, 2014; Radbourne et al., 2017). We suggest that calcite deposited during spring 2010 and autumn 2011 is likely to be particularly isotopically light, beyond the systematic offset noted above (samples RM83, RM113 and RM136; Table 2). Calcite found in traps at these times is fresh material rather than resuspended, as these are periods of high net ecosystem production (NEP; Scott, 2014), organic flux and positive calcite saturation index indicating supersaturation and rapid calcite precipitation (Fig. 2; Scott, 2014). If $\delta^{18}\text{O}_{\text{calcite}}$ values for these samples are adjusted by -0.9% (the average of the Baldeggersee and Sopensee offsets found by Teranes et al., 1999a; Teranes et al., 1999b and discussed above), they fall close to the regression line of the other 14 samples (Fig. 6a).

5.3.2. Towards developing a silica-calcite $\delta^{18}\text{O}$ geothermometer: potential and problems

With the caveats above, we explore the potential to develop an isotopic geothermometer at Rostherne Mere using data from the two-year monitoring period. Comparing $\delta^{18}\text{O}_{\text{calcite}}$ and $\delta^{18}\text{O}_{\text{diatom}}$, where both lake water $\delta^{18}\text{O}$ and temperature are known, provides independent assessments of the role of temperature on the signals in the different hosts. Several studies have looked at both within a sediment sequence (e.g. Lamb et al., 2005; Rozanski et al., 2010) but as far as we are aware, there are no published studies where both are analysed for contemporary material. This approach highlights the potential and the problems of each as a palaeoenvironmental proxy, as the two proxies represent conditions at different times of the year, and are subject to different sources of error ($\pm 0.1\%$ for $\delta^{18}\text{O}_{\text{calcite}}$ vs $\pm 0.3\%$ for $\delta^{18}\text{O}_{\text{diatom}}$, mainly due to analytical problems arising from contamination and the hydrous layer for diatom silica $\delta^{18}\text{O}_{\text{diatom}}$ analysis; Leng and Sloane, 2008). The $\delta^{18}\text{O}_{\text{diatom}}$ data fit with published fractionation relationships when plotted as $\ln \alpha_{(\text{host-water})}$ against temperature, where $\alpha_{(\text{host-water})} = (1000 + \delta^{18}\text{O}_{\text{host}}) / (1000 + \delta^{18}\text{O}_{\text{water}})$, the diatom data falling close to the line for cultured, recent and sediment trap lake data (Brandriss et al., 1998; Moschen et al., 2005; Crespin et al., 2010; Dodd and Sharp, 2010; Fig. 6a and b). Theoretical temperature values from $\delta^{18}\text{O}_{\text{calcite}}$ and $\delta^{18}\text{O}_{\text{diatom}}$ were calculated using the lake surface (0.5 m) $\delta^{18}\text{O}$ for that sample period and compared to measured temperatures using the equation of Kim and O'Neil (1997) for $\delta^{18}\text{O}_{\text{calcite}}$, and Moschen et al. (2005) for $\delta^{18}\text{O}_{\text{diatom}}$.

As expected, given the systematically lower values of $\delta^{18}\text{O}_{\text{calcite}}$, calculated $\delta^{18}\text{O}_{\text{calcite}}$ temperature overestimates observed temperature on average by $\sim 5^\circ\text{C}$ (Fig. 6a), similar to the overestimation ($+4.2^\circ\text{C}$) from contemporary (sediment trap) $\delta^{18}\text{O}_{\text{calcite}}$ found for a freshwater

lake in central Poland (Rozanski et al., 2010), also using the equation of Kim and O'Neil (1997). Rozanski et al. (2010) suggested that kinetic fractionation effects during rapid calcite precipitation produced bulk calcite with systematically lower $\delta^{18}\text{O}$ values than ambient water $\delta^{18}\text{O}$ values, leading to this calculated temperature offset. At Rostherne Mere, this may also partly be an artefact of using the average temperature over the upper 4 m whereas calcite precipitation may be occurring in the uppermost 1–2 m in association with the densest phytoplankton blooms (Scott, 2014; Radbourne, 2018), where temperatures are slightly higher (e.g. the difference between average temperatures in the upper 4 m and at 1 m is about 1 °C, and higher in summer, with a maximum of 2.7 °C in 2009).

On the seasonal timescales of this study, there are many potential sources of error in inferring temperature from $\delta^{18}\text{O}_{\text{diatom}}$ given the unresolved complexities in processes of silica precipitation, maturation and diatom taphonomy (dissolution and resuspension; Fig. 7) that additionally affect the $\delta^{18}\text{O}_{\text{diatom}}$ signal, as discussed above (e.g. Moschen et al., 2006; Dodd and Sharp, 2010; Dodd et al., 2012; Smith et al., 2016). Nevertheless, the trend to lower $\delta^{18}\text{O}_{\text{diatom}}$ in both the deep and shallow trap during spring/summer 2011 (though offset from each other; Fig. 5b) is in line with the fractionation expected as ambient upper lake temperatures rise over this period (-0.2‰ per 1 °C rise in temperature; Brandriss et al., 1998; Moschen et al., 2005; Crespin et al., 2010; Dodd and Sharp, 2010). Our shallow trap data are most comparable with the study of Moschen et al. (2005) at Lake Holzmaar, as expected given the similarities of the lakes and trapping approach (Fig. 6b). This study developed a $\delta^{18}\text{O}_{\text{diatom}}$ -temperature relationship using diatoms from the 7 m shallow trap (as higher values of $\delta^{18}\text{O}_{\text{diatom}}$ were observed in Holzmaar's deep trap samples, as in Rostherne Mere), and we refer to these data in the discussion below.

It is likely that at both Rostherne and Holzmaar, diatom silica from the traps has not reached equilibrium with ambient (trap) water, as the silica-water fractionation relationship is not at equilibrium (Fig. 6b). Contrary to conclusions reported by Dodd et al. (2012), more recent research suggests that the maturation process of silica, by dehydroxylation of silanols and the formation of siloxane through condensation, may take decades or centuries rather than months (Dodd et al., 2017), progressively altering $\delta^{18}\text{O}_{\text{diatom}}$ values. Using Eq. (5) below and considering the combined $\delta^{18}\text{O}_{\text{diatom}} \sim \delta^{18}\text{O}_{\text{calcite}}$ values, it might be possible to explore the extent to which this process has progressed, by estimating the amount of re-equilibrated silica in diatom samples. Given the range of factors involved in the kinetics of both diatom and calcite $\delta^{18}\text{O}$, and the few samples available here where both are measured, fuller investigation of this relationship is outside the scope of the present study.

Nonetheless, despite possible effects of rapid early maturation (Dodd et al., 2012; Dodd et al., 2017), the trend within the shallow trap $\delta^{18}\text{O}_{\text{diatom}}$ data is consistent with changes in lake temperature over a seasonal cycle and shows a strong and significant relationship to surface temperature. The equation of Moschen et al. (2005) fits observed temperature extremely well with almost no offset, suggesting a similar point has been reached on the maturation continuum in both cases (Dodd et al., 2017): $T_{\text{diatom}} (\text{°C}) = 0.943(T_{\text{obs}}) - 0.044$ ($r^2 = 0.60$, $p = 0.036$, $n = 6$). The best fit is with average daylight (0600–1800) temperatures in the upper 6 m, offset from the trap dates by 1 week (Table 3), reflecting the dominant process of light-driven biomineralisation of diatom silica within the mixed upper epilimnion, with an offset of about a week before senescent diatoms sediment into the upper trap at 10 m depth. There is clearly a blurring of this temperature signal as the seston moves down the water column, because the relationship is weaker, but still significant, in the deep-trap samples ($r^2 = 0.45$, $p = 0.034$, $n = 8$), leading to overestimation of epilimnion temperatures, like in other studies using surface-sediment data (Juillet-Leclerc and Labeyrie, 1987; Rietti-Shati et al., 1998). In the light of these results, we advise caution in using diatom silica $\delta^{18}\text{O}$ data for systems where maturation and dissolution effects have not been considered or

are unknown. Where the main purpose of applying $\delta^{18}\text{O}_{\text{diatom}}$ analysis is for palaeotemperature inference, we recommend (1) that samples covering several years are used to reduce within-year variability; and (2) that other independent proxies of temperature are used to build a consensus (for example to generate an envelope of most likely temperature range).

Combining $\delta^{18}\text{O}_{\text{calcite}}$ with known surface lake water $\delta^{18}\text{O}$ ($\delta^{18}\text{O}_{\text{lake}}$) opens up the possibility to generate equations to estimate seasonal lake epilimnion temperature from known $\delta^{18}\text{O}_{\text{calcite}}$ and $\delta^{18}\text{O}_{\text{diatom}}$, if the separate relationships for each host against temperature are known (Rozanski et al., 2010), with similar seasonality in production of diatom silica and calcite. The equation of Kim and O'Neil (1997) is re-expressed by Leng and Marshall (2004):

$$T_{\text{calcite}} (\text{°C}) = 13.8 - 4.58 (\delta^{18}\text{O}_{\text{calcite}} - \delta^{18}\text{O}_{\text{lake}}) + 0.08 (\delta^{18}\text{O}_{\text{calcite}} - \delta^{18}\text{O}_{\text{lake}})^2 \quad (1)$$

To simplify subsequent substitution of the $\delta^{18}\text{O}_{\text{lake}}$ term, we simplified Eq. (1) by ignoring the squared term, which did not reduce its predictive power. The fit to Rostherne data from Fig. 7b, without the squared term in Eq. (1), based on measured vs estimated temperature from Table 2, is $T_{\text{calcite}} = 1.060 T_{\text{lake}} + 4.388$ ($r^2 = 0.713$, $p < 0.0001$), where T_{lake} is the average (summer) temperature of the 0–4 m layer, corresponding to the trap period (which gave the best correlation for calcite; Table 2). For further simplicity in generating a combined diatom-calcite geothermometer, assuming the slope between T_{calcite} and $T_{\text{lake}} = 1$, rearranging this simplified Eq. (1) with respect to T_{lake} gives:

$$T_{\text{lake}} (\text{°C}) = 9.41 - 4.58 (\delta^{18}\text{O}_{\text{calcite}} - \delta^{18}\text{O}_{\text{lake}}) \quad (2)$$

The relationship of Moschen et al. (2005) provides a means to isolate $\delta^{18}\text{O}_{\text{lake}}$ if $\delta^{18}\text{O}_{\text{diatom}}$ is known, with the best fit for the daylight 0–6 m layer (see above):

$$T_{\text{diatom}} (\text{°C}) = 190.7 - 5.05 (\delta^{18}\text{O}_{\text{diatom}} - \delta^{18}\text{O}_{\text{lake}}) \quad (3)$$

Lake temperature data show that summer temperatures are 2.91 °C warmer on average in the upper 4 m compared to the daylight upper 6 m due to stratification ($r^2 = 0.971$ within the $\delta^{18}\text{O}_{\text{diatom}}$ dataset), i.e. $T_{\text{diatom}} + 2.91 = T_{\text{lake}}$ in Eq. (2). Using this correction for Rostherne in Eq. (3) so that both proxies ($\delta^{18}\text{O}_{\text{calcite}}$ and $\delta^{18}\text{O}_{\text{diatom}}$) refer to the same lake temperature target, summer surface (0–4 m) lake water temperature can be estimated from $\delta^{18}\text{O}_{\text{diatom}}$ as:

$$T_{\text{lake}} (\text{°C}) = 187.79 - 5.05 (\delta^{18}\text{O}_{\text{diatom}} - \delta^{18}\text{O}_{\text{lake}}) \quad (4)$$

Rearranging for $\delta^{18}\text{O}_{\text{lake}}$, substituting into Eq. (2) and simplifying gives an estimate for lake temperature (0–4 m) that does not rely on knowing $\delta^{18}\text{O}_{\text{lake}}$:

$$T_{\text{lake}} (\text{°C}) = 10. [(4.921 (\delta^{18}\text{O}_{\text{diatom}} - \delta^{18}\text{O}_{\text{calcite}}) - 172.27)] \quad (5)$$

Unfortunately, too few samples with both $\delta^{18}\text{O}_{\text{diatom}}$ and $\delta^{18}\text{O}_{\text{calcite}}$ are available to test the geothermometer of Eq. (5) rigorously from our dataset, but it is clear that Eq. (5) will be very sensitive to errors in the difference of ($\delta^{18}\text{O}_{\text{diatom}} - \delta^{18}\text{O}_{\text{calcite}}$), as an error of $\pm 0.1\text{‰}$ in ($\delta^{18}\text{O}_{\text{diatom}} - \delta^{18}\text{O}_{\text{calcite}}$) will result in a temperature difference of ca. ± 5 °C.

More fundamentally, our results suggest that a universally applicable diatom-calcite $\delta^{18}\text{O}$ relationship for palaeoclimate inference will be very difficult to develop. Whereas there might be potential in exploring such a dual isotope geothermometer, our study shows that great caution must be exercised in any such attempts, particularly given the impact of disequilibrium fractionation on $\delta^{18}\text{O}_{\text{calcite}}$ values in lakes where calcite precipitation is rapid, and long-term diagenetic (dehydroxylation) changes that occur within diatom silica, which may override a temperature imprint. Before a diatom-calcite geothermometer can be developed and applied to sedimentary data in a given

lake, it is fundamental to understand contemporary $\delta^{18}\text{O}_{\text{diatom}}$ and $\delta^{18}\text{O}_{\text{calcite}}$ dynamics and processes within that system, considering the range of possible factors affecting $\delta^{18}\text{O}$ values from seston to sediment. Furthermore, calcite precipitation dynamics may vary as a lake trophic status changes (e.g. progressively isotopically lighter calcite may precipitate in lakes undergoing eutrophication; Fronval et al., 1995; Teranes et al., 1999b), an increasingly common trajectory for freshwater lakes globally. This implies that, in such cases, monitoring of the contemporary isotopic system may not be an analogue for the lake under less eutrophic conditions in the past. Until these issues are addressed and quantified, although each proxy might individually contain palaeotemperature information, the prospect of developing an accurate and reliable geothermometer from paired $\delta^{18}\text{O}_{\text{diatom}}$ and $\delta^{18}\text{O}_{\text{calcite}}$ will remain elusive.

6. Conclusions

High resolution and multi-annual monitoring of both endogenic calcite and diatom deposition from sediment traps can be used to explore the environmental controls over oxygen isotope ratios in lacustrine water, biogenic silica and calcite. In a study of Rostherne Mere, both calcite and diatom $\delta^{18}\text{O}$ were found to be out of isotopic equilibrium. For calcite, we suggest this is largely due to rapid calcite precipitation in meso-eutrophic systems, although there was no apparent effect of calcite dissolution, despite both shallow and deep traps lying in waters undersaturated with respect to calcite. Variations in $\delta^{18}\text{O}_{\text{diatom}}$ are more complex, with evidence that there is a rapid alteration (and an enrichment of about +0.7‰; Fig. 5b) of the diatom silica frustule $\delta^{18}\text{O}$ value within weeks after death and sedimentation. We speculate that this post-mortem maturation is linked to the time valves are exposed to anoxic conditions, and to the effects of anaerobic bacteria on the fresh silica matrix. Additionally, dissolution may result in changes to $\delta^{18}\text{O}$ values, leading to significant, but potentially predictable, error in temperatures inferred using the diatom $\delta^{18}\text{O}$ proxy. The intriguing findings presented here from the well-characterised natural laboratory of Rostherne Mere can form the basis for further work, for example through experimentation on fresh diatom material.

Monitoring for more than an annual cycle also shows that the seasonal cycle and inter-annual variations in lake water $\delta^{18}\text{O}$ and temperature may not always be clearly recorded in lacustrine (endogenic) $\delta^{18}\text{O}_{\text{calcite}}$ and $\delta^{18}\text{O}_{\text{diatom}}$. Whereas our study does give some support to their use as palaeoclimatic proxies individually (with the caveats above), major obstacles in our understanding remain before paired diatom-calcite $\delta^{18}\text{O}$ can be used directly as a robust geothermometer, even in a well-understood system such as Rostherne Mere. Although a temperature signal may be captured at the point of host formation of both $\delta^{18}\text{O}_{\text{diatom}}$ and $\delta^{18}\text{O}_{\text{calcite}}$, this imprint is subject to alteration and diagenesis almost immediately, in ways which are as yet incompletely understood. This is especially the case for diatom silica, which undergoes both rapid and potentially longer-term alteration affecting the quality of the $\delta^{18}\text{O}_{\text{diatom}}$ signal as the fossil diatom assemblage dissolves and ages. Bridging this gap in understanding between processes occurring within the isotope host at the timescale of weeks and months, and those occurring over longer timescales (from decades to geological timespans) as the signal is incorporated into the sedimentary archive, is key to developing these proxies further both individually, and potentially together, as palaeoclimatic tools.

Declaration of competing interest

The authors declare that they have no known competing financial interests or personal relationships that could have appeared to influence the work reported in this paper.

Acknowledgements

This work was carried out under a NERC award (NE/H011978/1 to DBR, MJL and JJT), and supported by NERC Geosciences Steering Committee awards (IP-1181-0510, IP-1256-0511 and IP-1319-0512) for O and H isotope analyses. JJT was supported by NERC Fellowship NE/F014708/1. DRS was supported by the Loughborough University Development Fund during a PhD. We thank Natural England for access to Rostherne Mere and help with fieldwork and logistics, especially Sarah Warrenner and Rupert Randall, and field assistance from Andrew Pledger, Jon Lewis, Iestyn Woolway, Stuart Ashby, Barry Kenny and Chris Goldspink. Members of the Centre for Hydrology and Ecology (CEH) at Lancaster are thanked for their generous assistance with the UKLEON buoy at Rostherne, especially Jack Kelly, Mike Clarke, Ben James (fieldwork) and Martin Rouen (for data access), supported within a NERC Network of Sensors award (NE/I007261 to DBR and NE/I007407/1 to CEH). Additional data (e.g. temperature datasets, water isotope data) used within this study will be made freely available in the National Geoscience Data Centre (NGDC; <https://www.bgs.ac.uk/services/NGDC/home.html>) for geoscientific data and information. We thank Michael Böttcher, Alfonso Mucci, Justin Dodd and four anonymous reviewers for their insightful and valuable comments that led to significant improvements of the manuscript.

References

- APHA, 2005. Standard Methods for the Examination of Water and Wastewater, 21st ed. American Public Health Association/American Water Works Association/Water Environment Federation, Washington, D.C.
- Bailey, H.L., Henderson, A.C.G., Sloane, H.J., Snelling, A., Leng, M.J., Kaufman, D.S., 2014. The effect of species on lacustrine delta O-18(diatom) and its implications for palaeoenvironmental reconstructions. *J. Quat. Sci.* 29, 393–400.
- Bidle, K., Azam, F., 1999. Accelerated dissolution of diatom silica by marine bacterial assemblages. *Nature* 397, 508–512. <https://doi.org/10.1038/17351>.
- Bluszcz, P., Lücke, A., Ohlendorf, C., Zolitschka, B., 2009. Seasonal dynamics of stable isotopes and element ratios in authigenic calcites during their precipitation and dissolution, Sacrower See (northeastern Germany). *J. Limnol.* 68, 257–273.
- Brandriss, M.E., O'Neil, J.R., Edlund, M.B., Stoermer, E.F., 1998. Oxygen isotope fractionation between diatomaceous silica and water. *Geochim. Cosmochim. Acta* 62, 1119–1125.
- Carvalho, L.R., 1993. Experimental Limnology on Four Cheshire Meres. University of Liverpool, pp. 385.
- Carvalho, L., Beklioglu, M., Moss, B., 1995. Changes in a deep lake following sewage diversion - a challenge to the orthodoxy of external phosphorus control as a restoration strategy. *Freshw. Biol.* 34, 399–410.
- Chapligin, B., Leng, M.J., Webb, E., Alexandre, A., Dodd, J.P., Ijiri, A., Lücke, A., Shemesh, A., Abelmann, A., Herzschiuh, U., Longstaffe, F.J., Meyer, H., Moschen, R., Okazaki, Y., Rees, N.H., Sharp, Z.D., Sloane, H.J., Sonzogni, C., Swann, G.E.A., Sylvestre, F., Tyler, J.J., Yam, R., 2011. Inter-laboratory comparison of oxygen isotopes from biogenic silica. *Geochim. Cosmochim. Acta* 75, 7242–7256.
- Chapligin, B., Meyer, H., Bryan, A., Snyder, J., Kennitz, H., 2012. Assessment of purification and contamination correction methods for analysing the oxygen isotope composition from biogenic silica. *Chem. Geol.* 300, 185–199.
- Coplen, T.B., 1995. Discontinuance of SMOW and PDB. *Nature* 375, 285. <https://doi.org/10.1038/375285a0>.
- Coplen, T.B., 2007. Calibration of the calcite-water oxygen-isotope geothermometer at Devils Hole, Nevada, a natural laboratory. *Geochim. Cosmochim. Acta* 71, 3948–3957.
- Coplen, T., Kendall, C., Hopple, J., 1983. Comparison of stable isotope reference samples. *Nature* 302, 236–238.
- Crespin, J., Sylvestre, F., Alexandre, A., Sonzogni, C., Pailles, C., Perga, M.E., 2010. Re-examination of the temperature-dependent relationship between $\delta\text{O}^{18}_{\text{diatoms}}$ and $\delta\text{O}^{18}_{\text{lake water}}$ and implications for paleoclimate inferences. *J. Paleolimnol.* 44, 547–557.
- Daëron, M., Drysdale, R.N., Peral, M., Huyghe, D., Blamart, D., Coplen, T.B., Lartaud, F., Zanchetta, G., 2019. Most Earth-surface calcites precipitate out of isotopic equilibrium. *Nat. Commun.* 10, 429.
- Dean Jr., W.E., 1974. Determination of carbonate and organic matter in calcareous sediments and sedimentary rocks by loss-on-ignition: comparison with other methods. *J. Sediment. Petrol.* 44, 242–248.
- Dean, J.R., Jones, M.D., Leng, M.J., Sloane, H.J., Roberts, C.N., Woodbridge, J., Swann, G.E.A., Metcalfe, S.E., Eastwood, W.J., Yigitbasioğlu, H., 2013. Palaeo-seasonality of the last two millennia reconstructed from the oxygen isotope composition of carbonates and diatom silica from Nar Golu, central Turkey. *Quat. Sci. Rev.* 66, 35–44.
- Dean, J.R., Eastwood, W.J., Roberts, N., Jones, M.D., Yigitbasioğlu, H., Allcock, S.L., Woodbridge, J., Metcalfe, S.E., Leng, M.J., 2015. Tracking the hydro-climatic signal from lake to sediment: a field study from central Turkey. *J. Hydrol.* 529, 608–621.
- Dodd, J.P., Sharp, Z.D., 2010. A laser fluorination method for oxygen isotope analysis of biogenic silica and a new oxygen isotope calibration of modern diatoms in freshwater

- environments. *Geochim. Cosmochim. Acta* 74, 1381–1390.
- Dodd, J.P., Sharp, Z.D., Fawcett, P.J., Brearley, A.J., McCubbin, F.M., 2012. Rapid post-mortem maturation of diatom silica oxygen isotope values. *Geochim. Geophys. Geosyst.* 13.
- Dodd, J.P., Wiedenheft, W., Schwartz, J.M., 2017. Dehydroxylation and diagenetic variations in diatom oxygen isotope values. *Geochim. Cosmochim. Acta* 199, 185–195.
- Fronval, T., Jensen, N.B., Buchardt, B., 1995. Oxygen-isotope disequilibrium precipitation of calcite in Lake Arreso, Denmark. *Geology* 23, 463–466.
- Grimshaw, H.M., Hudson, M.J., 1970. Some mineral nutrient studies of a lowland mere in Cheshire, England. *Hydrobiologia* 36, 329–341.
- Hargreaves, K.R., Anderson, N.J., Clokie, M.R.J., 2013. Recovery of viable cyanophages from the sediments of a eutrophic lake at decadal timescales. *FEMS Microbiol. Ecol.* 83, 450–456.
- Hodell, D.A., Schelske, C.L., Fahnenstiel, G.L., Robbins, L.L., 1998. Biologically induced calcite and its isotopic composition in Lake Ontario. *Limnol. Oceanogr.* 43, 187–199.
- Juillet-Leclerc, A., Labeyrie, L., 1987. Temperature-dependence of the oxygen isotopic fractionation between diatom silica and water. *Earth Planet. Sci. Lett.* 84, 69–74.
- Kim, S.T., O'Neil, J.R., 1997. Equilibrium and nonequilibrium oxygen isotope effects in synthetic carbonates. *Geochim. Cosmochim. Acta* 61, 3461–3475.
- Krivtsov, V., Sigeo, D., Bellinger, E., 2001. A one-year study of the Rostherne Mere ecosystem: seasonal dynamics of water chemistry, plankton, internal nutrient release, and implications for long-term trophic status and overall functioning of the lake. *Hydro. Process.* 15, 1489–1506.
- Lamb, A.L., Leng, M.J., Sloane, H.J., Telford, R.J., 2005. A comparison of the palaeoclimate signals from diatom oxygen isotope ratios and carbonate oxygen isotope ratios from a low latitude crater lake. *Palaeogeogr. Palaeoclimatol. Palaeoecol.* 223, 290–302.
- Leng, M.J., Marshall, J.D., 2004. Palaeoclimate interpretation of stable isotope data from lake sediment archives. *Quat. Sci. Rev.* 23, 811–831.
- Leng, M.J., Sloane, H.J., 2008. Combined oxygen and silicon isotope analysis of biogenic silica. *J. Quat. Sci.* 23, 313–319.
- Li, D., Han, J., 2010. Temperature-induced fractionation of oxygen isotopes of diatom frustules and growth water in Lake Sihailongwan in Northeast China. *Chin. Sci. Bull.* 55, 3794–3801.
- Livingstone, D., Reynolds, C.S., 1981. Algal sedimentation in relation to phytoplankton periodicity in Rostherne Mere. *Br. Phycol. J.* 16, 195–206.
- Martin-Jezequel, V., Hildebrand, M., Brzezinski, M.A., 2000. Silicon metabolism in diatoms: implications for growth. *J. Phycol.* 36, 821–840.
- Miklasz, K.A., Denny, M.W., 2010. Diatom sinking speeds: improved predictions and insight from a modified Stokes' law. *Limnol. Oceanogr.* 55, 2513–2525.
- Morley, D.W., Leng, M.J., Mackay, A.W., Sloane, H.J., Rioual, P., Battarbee, R.W., 2004. Cleaning of lake sediment samples for diatom oxygen isotope analysis. *J. Paleolimnol.* 31, 391–401.
- Moschen, R., Lücke, A., Schleser, G.H., 2005. Sensitivity of biogenic silica oxygen isotopes to changes in surface water temperature and palaeoclimatology. *Geophys. Res. Lett.* 32, 4.
- Moschen, R., Lücke, A., Parplies, J., Radtke, U., Schleser, G.H., 2006. Transfer and early diagenesis of biogenic silica oxygen isotope signals during settling and sedimentation of diatoms in a temperate freshwater lake (Lake Holzmaar, Germany). *Geochim. Cosmochim. Acta* 70, 4367–4379.
- Moss, B., Barker, T., Stephen, D., Williams, A.E., Balayla, D.J., Beklioglu, M., Carvalho, L., 2005. Consequences of reduced nutrient loading on a lake system in a lowland catchment: deviations from the norm? *Freshw. Biol.* 50, 1687–1705.
- Ohlendorf, C., Sturm, M., 2001. Precipitation and dissolution of calcite in a Swiss High Alpine Lake. *Arct. Antarct. Alp. Res.* 33, 410–417.
- Prentice, A.J., Webb, E.A., 2016. The effect of progressive dissolution on the oxygen and silicon isotope composition of opal-A phytoliths: implications for palaeoenvironmental reconstruction. *Palaeogeogr. Palaeoclimatol. Palaeoecol.* 453, 42–51.
- Radbourne, Alan D., 2018. Disentangling the impacts of nutrient enrichment and climatic forcing as key drivers of change at Rostherne Mere. Loughborough University. Thesis. <https://hdl.handle.net/2134/34927>.
- Radbourne, A.D., Ryves, D.B., Anderson, N.J., Scott, D.R., 2017. The historical dependency of organic carbon burial efficiency. *Limnol. Oceanogr.* 62, 1480–1497.
- Raubitschek, S., Lücke, A., Schleser, G.H., 1999. Sedimentation patterns of diatoms in Lake Holzmaar, Germany - (on the transfer of climate signals to biogenic silica oxygen isotope proxies). *J. Paleolimnol.* 21, 437–448.
- Reynolds, C.S., 1978. Notes on phytoplankton periodicity of Rostherne Mere, Cheshire, 1967–1977. *Br. Phycol. J.* 13, 329–335.
- Reynolds, C.S., 1979. The limnology of the eutrophic meres of the Shropshire-Cheshire Plain. *Field Stud.* 5, 93–173.
- Riotti-Shati, M., Shemesh, A., Karlen, W., 1998. A 3000-year climatic record from biogenic silica oxygen isotopes in an equatorial high-altitude lake. *Science* 281, 980–982.
- Rozanski, K., Klisch, M.A., Wachniew, P., Gorczyca, Z., Goslar, T., Edwards, T.W.D., Shemesh, A., 2010. Oxygen-isotope geothermometers in lacustrine sediments: new insights through combined delta O-18 analyses of aquatic cellulose, authigenic calcite and biogenic silica in Lake Goszcz, central Poland. *Geochim. Cosmochim. Acta* 74, 2957–2969.
- Ryves, D.B., Juggins, S., Fritz, S.C., Battarbee, R.W., 2001. Experimental diatom dissolution and the quantification of microfossil preservation in sediments. *Palaeogeogr. Palaeoclimatol. Palaeoecol.* 172, 99–113.
- Ryves, D.B., Jewson, D.H., Sturm, M., Battarbee, R.W., Flower, R.J., Mackay, A.W., Granin, N., 2003. Quantitative and qualitative relationships between planktonic diatom communities and diatom assemblages in sedimenting material and surface sediments in Lake Baikal, Siberia. *Limnol. Oceanogr.* 48, 1643–1661.
- Ryves, D.B., Battarbee, R.W., Juggins, S., Fritz, S.C., Anderson, N.J., 2006. Physical and chemical predictors of diatom dissolution in freshwater and saline lake sediments in North America and West Greenland. *Limnol. Oceanogr.* 51, 1355–1368. <https://doi.org/10.4319/lo.2006.51.3.1355>.
- Ryves, D.B., Anderson, N.J., Flower, R.J., Rippey, B., 2013. Diatom taphonomy and silica cycling in two freshwater lakes and their implications for inferring past lake productivity. *J. Paleolimnol.* 49, 411–430.
- Schmidt, M., Botz, R., Rickert, D., Bohrmann, G., Hall, S.R., Mann, S., 2001. Oxygen isotopes of marine diatoms and relations to opal-A maturation. *Geochim. Cosmochim. Acta* 65, 201–211.
- Scott, Daniel R., 2014. Carbon fixation, flux and burial efficiency in two contrasting eutrophic lakes in the UK (Rostherne Mere & Tatton Mere). Loughborough University. Thesis. <https://hdl.handle.net/2134/16949>.
- Shemesh, A., Burckle, L.H., Froelich, P.N., 1989. Dissolution and preservation of Antarctic diatoms and the effect on sediment thanatocones. *Quaternary Research* 31 (2), 288–308. [https://doi.org/10.1016/0033-5894\(89\)90010-0](https://doi.org/10.1016/0033-5894(89)90010-0).
- Shemesh, A., Charles, C.D., Fairbanks, R.G., 1992. Oxygen isotopes in biogenic silica: global changes in ocean temperature and isotopic composition. *Science* 256, 1434–1436.
- Smith, A.C., Leng, M.J., Swann, G.E.A., Barker, P.A., Mackay, A.W., Ryves, D.B., Sloane, H.J., Chenery, S.R.N., Hems, M., 2016. An experiment to assess the effects of diatom dissolution on oxygen isotope ratios. *Rapid Commun. Mass Spectrom.* 30, 293–300.
- Stansell, N.D., Klein, E.S., Finkenbinder, M.S., Fortney, C.S., Dodd, J.P., Terasmaa, J., Nelson, D.B., 2017. A stable isotope record of Holocene precipitation dynamics in the Baltic region from Lake Nuudsaku, Estonia. *Quat. Sci. Rev.* 175, 73–84.
- Swann, G.E.A., Leng, M.J., Sloane, H.J., Maslin, M.A., Onodera, J., 2007. Diatom oxygen isotopes: evidence of a species effect in the sediment record. *Geochim. Geophys. Geosyst.* 8.
- Swann, G.E.A., Leng, M.J., Juschus, O., Melles, M., Brigham-Grette, J., Sloane, H.J., 2010. A combined oxygen and silicon diatom isotope record of Late Quaternary change in Lake El'gygytgyn, North East Siberia. *Quat. Sci. Rev.* 29, 774–786.
- Tattersall, W.M., Coward, T.A., 1914. Faunal survey of Rostherne Mere. I. Introduction and methods. In: *Memoirs of the Proceedings of the Manchester Literary and Philosophical Society.* 58, pp. 1–21.
- Teranes, J.L., McKenzie, J.A., Bernasconi, S.M., Lotter, A.F., Sturm, M., 1999a. A study of oxygen isotopic fractionation during bio-induced calcite precipitation in eutrophic Baldeggsee, Switzerland. *Geochim. Cosmochim. Acta* 63, 1981–1989.
- Teranes, J.L., McKenzie, J.A., Lotter, A.F., Sturm, M., 1999b. Stable isotope response to lake eutrophication: calibration of a high-resolution lacustrine sequence from Baldeggsee, Switzerland. *Limnol. Oceanogr.* 44, 320–333.
- Tyler, J.J., Leng, M.J., Sloane, H.J., Sachse, D., Gleixner, G., 2008. Oxygen isotope ratios of sedimentary biogenic silica reflect the European transcontinental climate gradient. *J. Quat. Sci.* 23, 341–350.
- Tyler, J.J., Sloane, H.J., Rickaby, R.E.M., Cox, E.J., Leng, M.J., 2017. Post-mortem oxygen isotope exchange within cultured diatom silica. *Rapid Commun. Mass Spectrom.* 31, 1749–1760.
- van Hardenbroek, M., Chakraborty, A., Davies, K.L., Harding, P., Heiri, O., Henderson, A.C.G., Holmes, J.A., Lasher, G.E., Leng, M.J., Panizzo, V.N., Roberts, L., Schilder, J., Trueman, C.N., Wooller, M.J., 2018. The stable isotope composition of organic and inorganic fossils in lake sediment records: Current understanding, challenges, and future directions. *Quat. Sci. Rev.* 196, 154–176. <https://doi.org/10.1016/j.quascirev.2018.08.003>.
- Watkins, J.M., Hunt, J.D., Ryerson, F.J., DePaolo, D.J., 2014. The influence of temperature, pH, and growth rate on the delta O-18 composition of inorganically precipitated calcite. *Earth Planet. Sci. Lett.* 404, 332–343.
- Werner, D., 1977. *The Biology of Diatoms.* University of California Press, University of California Press.